2009-11-19

Synthesis and Evaluation of N6,5'-Bis-Ureido-5'-Amino-5'-Deoxyadenosine Derivatives: Novel Nucleosides with Antiproliferative and Protein Kinase Binding Activities

Marcelio Oliveira
Brigham Young University - Provo

Synthesis and Evaluation of N^6,5′-Bis-ureido-5′-amino-5′-deoxyadenosine Derivatives: Novel Nucleosides with Antiproliferative and Protein Kinase Binding Activities

by

Marcélio de Moura Oliveira

A thesis submitted to the faculty of
Brigham Young University
in partial fulfillment of the requirements for the degree of

Master of Science

Matt A. Peterson, Committee Chair
Young Wan Ham, Committee Member
Roger G. Harrison, Committee Member

Department of Chemistry and Biochemistry

Brigham Young University

December 2009

ABSTRACT

Synthesis and Evaluation of N^6,5′-Bis-ureido-5′-amino-5′-deoxyadenosine Derivatives: Novel Nucleosides with Antiproliferative and Protein Kinase Binding Activities

Marcélio de Moura Oliveira

Department of Chemistry and Biochemistry

Master of Science

A new series of N^6,5′-bis-ureido-5′-amino-5′-deoxyadenosine derivatives was prepared and evaluated for anticancer activities using the NCI 60 panel of human cancers. Certain of the derivatives showed promising activities (low micromolar GI_{50}'s) against several of the representative cancers. These included cell lines from the following general cell types in the NCI 60: Leukemia, Breast, Central Nervous System, Non-Small Cell Lung, Ovarian, Prostate, Renal, and Colon cancers. Select compounds were also screened for their affinities for protein kinases. The synthesis of the compounds was straightforward and involved N^6 acylation with arylisocyanates, preceded by activation and nucleophilic substitution of the 5′-position to give the desired 5′-azido-5′-deoxyadenosine derivatives. Reduction of the 5′-azido function with either H_2/Pd-C, or Ph_3P/H_2O, gave the desired 5′-amino-5′-deoxyadenosine products. Acylation of the 5′-amino group with *N*-methyl 4-nitrophenylcarbamate gave the N^6,5′-bis-ureido-5′-amino-5′-deoxyadenosine products. Yields ranged from good (50–75%) to excellent (75–95%) for all synthetic transformations.

Keywords: Anti-cancer agents, N^6,5'-bis-ureido deoxyadenosine, protein kinases

ACKNOWLEDGMENTS

I would like to thank my family for its support over the last two years. I would like to thank my friends and colleagues Jadd Shelton and Chris Cuttler for all their help in developing synthesis as well as their companionship. I would like to thank my friend and advisor Dr. Matt A. Peterson for all his instructions, kindness, patience and humor during our work together. I would like to thank Dr. Roger G. Harrison and Dr. Young Wan Ham for being members of my graduate committee. I'm grateful for all the help from Ms. Janet Fonoimoana in all the paperwork and in all the various administrative details that were necessary to be made until now. Finally, I would like to thank the Department of Chemistry and Biochemistry at BYU for the financial support that was used for the development of this work, as well as for providing the wonderful environment that was shared with me over the last two years.

Thanks to all.

TABLE OF CONTENTS

Table of Contents vii

List of Figures viii

List of Schemes ix

List of Tables x

Introduction 1

Background 4

Results and Discussion 16

Conclusion 24

Experimental Section 25

Appendix 42

References 50

LIST OF FIGURES

Figure 1. Structures of cancer-related protein kinase inhibitors Imatinib, Gefitinib, and Erlotinib……..……...2

Figure 2. Pharmacophore model of the ATP-binding site of protein kinases…..……3

Figure 3. Potential HIV integrase inhibitors prepared by Peterson et al…….4

Figure 4. 3'-End processing of viral DNA by HIV integrase…..……5

Figure 5. Strand transfer of viral DNA by HIV integrase ……..5

Figure 6. Putative binding of adenosine derivatives in the active site of HIV integrase…6

Figure 7. Inhibition of binding of protein kinases to ATP-binding site ligands by **1**…...11

Figure 8. Binding inhibition ≥ 30% observed in 11 of 353 protein kinases……..12

Figure 9. Selective inhibition of binding of Alk6 by compound **1**……...13

Figure 10. Selective inhibition of binding to p38 protein kinases by **1**……...13

Figure 11. Selective inhibition of binding to PAK protein kinases by **1**…….13

Figure 12. Inhibition of cancer-related protein kinases by compound **1**…….15

Figure 13. Quadrants for SAR of compound **1**……16

Figure 14. Targets for structure activity study (SAR)…….17

Figure 15. Structures of inventory compounds……...22

LIST OF SCHEMES

Scheme 1. Synthesis of compounds **9** and **10**…….18

Scheme 2. Synthesis of compound **11** …..…….18

Scheme 3. Synthetic targets for more in-depth SAR……...23

LIST OF TABLES

Table 1. Activities of test compounds in biochemical assays……..……6

Table 2. Results of single dose growth inhibition assay…….8

Table 3. Results of multi-dose inhibition assay for compound **1** ……...9

Table 4. Results of multi-dose inhibition assay for compound **2** …….10

Table 5. Single dose growth inhibition assay for **9** and **10**……21

Introduction

Protein kinases constitute a large family of homologous proteins involved with control of such key cellular processes as cell growth and differentiation, apoptosis, and signal transduction. Protein kinases catalyze phosphorylation of hydroxyl groups of serine, threonine, or tyrosine in a substrate protein. This phosphorylation is executed with transfer of the gamma phosphate group of ATP or GTP to the substrate protein. The phosphorylated protein then undergoes a series of binding events with downstream proteins, thus setting in motion the cascade of reactions typically involved in signal transduction. Signal transduction processes are extremely complex, with numerous instances of pathway "cross talk" and/or reversal of signal outcome that have been documented. The key role played by protein kinases in cell growth and differentiation has prompted their investigation as promising targets for anticancer drug design.[1] The high incidence of these enzymes in cancer cells corroborates their importance as interesting targets in cancer treatment and the correlation between their aberrant expression and tumorigenesis has been well documented.[2] In recent years, protein kinases have emerged as one of the most important targets for drug development research, and it is estimated that approximately 25% of all pharmaceutical research focuses on protein kinases.[3] Studies show that approximately 90% of patients with chronic myeloid leukemia (CML) exhibit a chromosomal defect that results in a hyper expression of certain kinases.[4] In addition, chemotherapy that targets protein kinases shows efficiency of about 90% when focused on inhibition of these enzymes.[5]

Some recently developed drugs that have been approved for cancer treatment that function as protein kinase inhibitors include Imatinib Mesilate (in chronic myeloid

leukemia);[6] Gefitinib (in non-small cell lung cancer);[7] and Erlotinib (in non-small cell lung cancer) (**Figure 1**).[8]

Figure 1. Structures of cancer-related protein kinase inhibitors Imatinib, Gefitinib and Erlotinib.

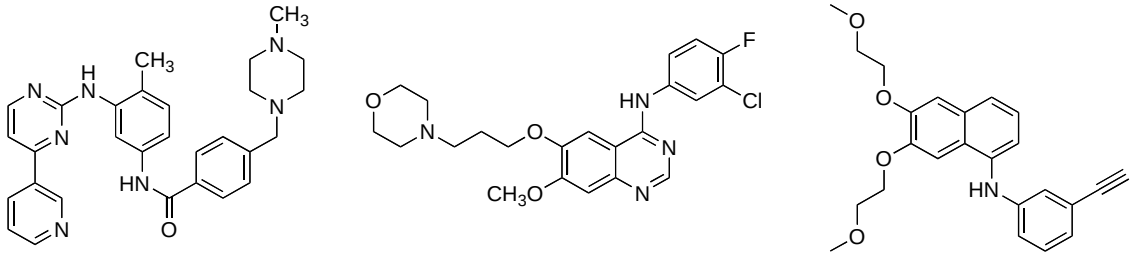

Among the various approaches to discovery of protein kinase inhibitors that have been evaluated to date, targeting the catalytic site with ATP-competitive inhibitors has proven most successful.[9] Other approaches involving non-competitive or allosteric inhibitors have met with much more limited success.[6] To date, over 50 crystal structures of protein kinases complexed with ATP site-directed inhibitors are now available, thus confirming the effectiveness of the ATP-binding site as a target for drug design.

The currently accepted pharmacophore model for the ATP-binding pocket of protein kinases is illustrated in Figure 2. This model consists of the following key features:

(1) Adenine binding region. This region consists of a bidentate hydrogen-bonding donor-acceptor motif in the hinge region. Hydrogen bonds between the protein backbone and N1 and N6 occur between a hinge region amide NH and carbonyl moiety, respectively. These interactions constitute the adenine anchoring interactions and many potent inhibitors exploit at least one of these hydrogen bond interactions.

(2) Hydrophobic pocket. This hydrophobic region flanks the region proximal to N6 of the adenine heterocycle. This pocket has been exploited by numerous inhibitors and plays an important role for inhibitor selectivity.

(3) Phosphate binding pocket. This pocket consists of positively charged amino acid residues such as lysine and/or arginine. Electrostatic interactions between the negatively charged phosphate and positively charged amino acid side chains occur in this region. This pocket appears to be the least important due to high solvent exposure, but it has been used to improve selectivity and gain additional binding affinity.

(4) Sugar binding region. This region, with very few exceptions, is hydrophilic and is designed to bind to the ribose hydroxyls through hydrogen-bond donor-acceptor interactions.

(5) Hyrophobic channel. This channel lies between the sugar binding and hinge regions and can exist in an open, solvent exposed, configuration. Since it is not utilized by ATP, it can be exploited to gain inhibitor binding affinity.

Figure 2. Pharmacophore model of the ATP-binding site of protein kinases.[9]

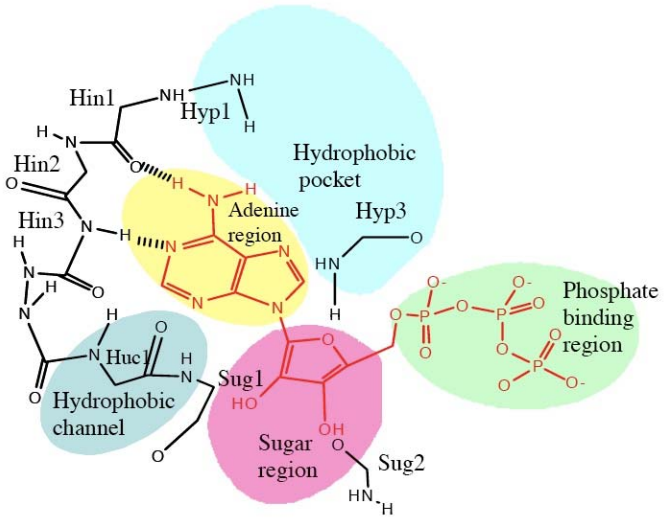

Background

Recently, N^6,5′-bis-ureidoadenosine compounds **1**–**7** were synthesized by Peterson et al. and select members of these compounds showed interesting cytotoxic properties against MT2 lymphoma cells in vitro (Figure 3).[10]

Figure 3. Potential HIV integrase inhibitors prepared by Peterson et al.

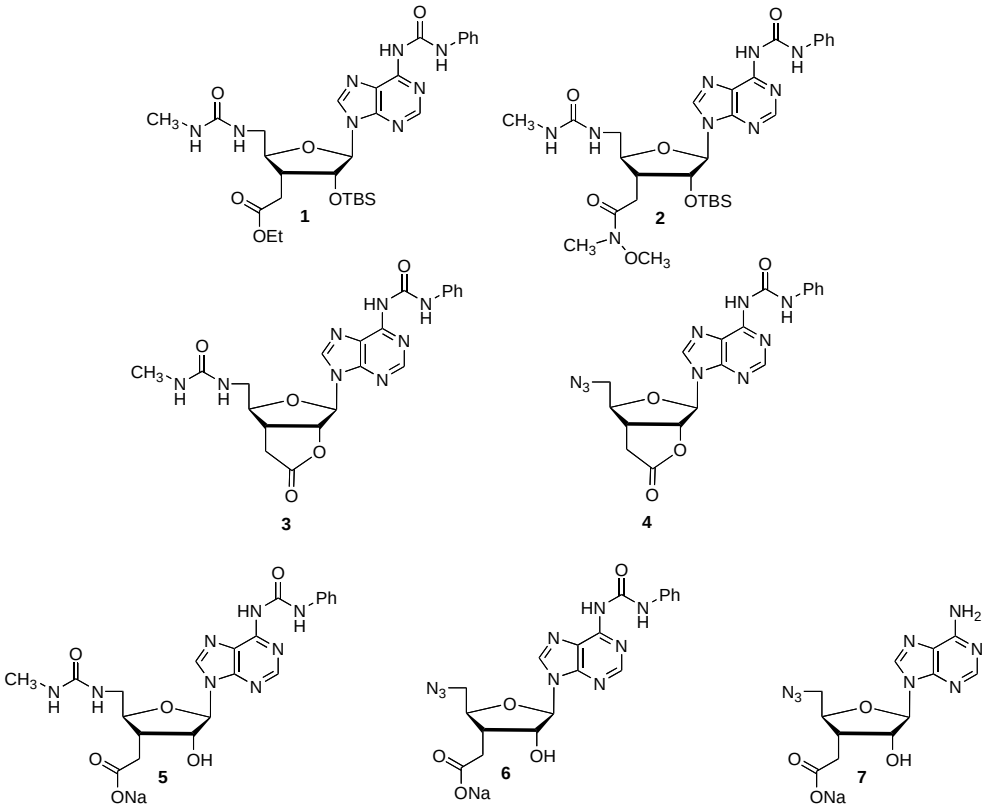

The original motivation for preparing these compounds was their potential utility as HIV integrase inhbitors. HIV integrase is one of three enzymes encoded for by HIV. These include reverse transcriptase, protease, and integrase. HIV integrase possesses two enzymatic activities: (1) 3′-end processing, and (2) strand transfer. Each activity involves an Mg^{2+}–promoted chemical reaction in which the Mg^{2+} and associated amino acid residues are in close proximity to the 3′-hydroxyl of a 2′-deoxyadenosine residue of the viral DNA substrate (Figures 4 and 5).

Figure 4. 3′-End processing of viral DNA by HIV integrase.

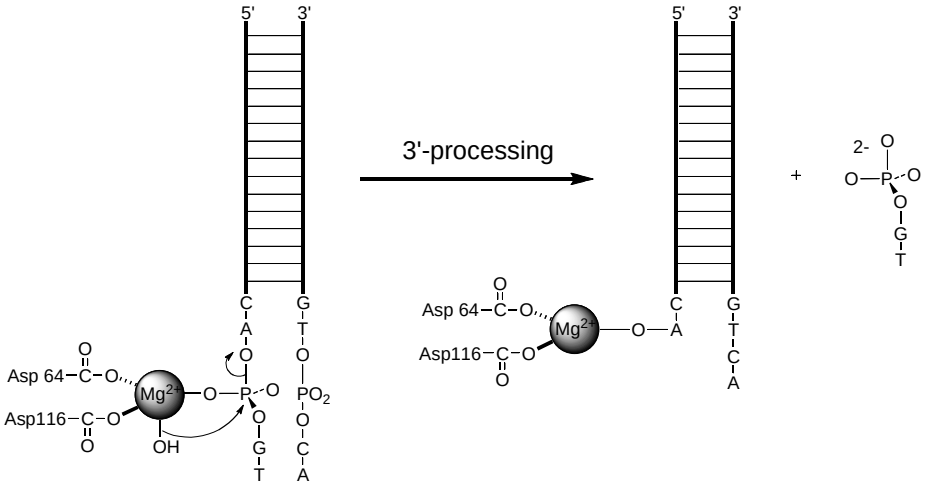

Figure 5. Strand transfer of viral DNA by HIV integrase.

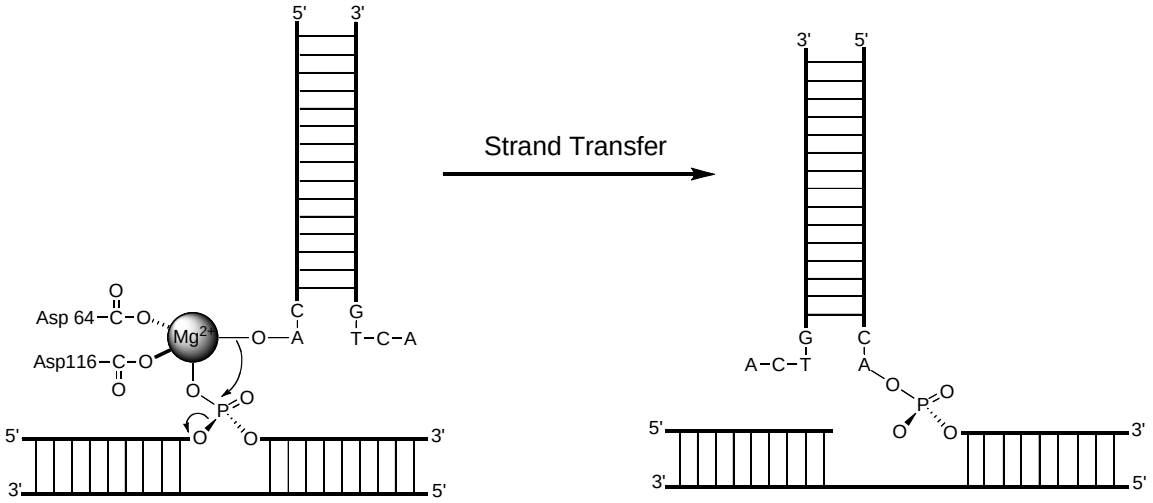

Peterson et al. reasoned that appropriately derivatized adenosine analogues with metal-binding moieties attached to the 3′-position might be expected to bind to the active site of HIV integrase and thus inhibit the enzyme (Figure 6). Unfortunately, compounds **1**–**7** were devoid of anti-HIV activity and failed to exhibit measurable inhibition of HIV integrase at the concentrations tested (Table 1).

Figure 6. Putative binding of adenosine derivatives in the active site of HIV integrase.

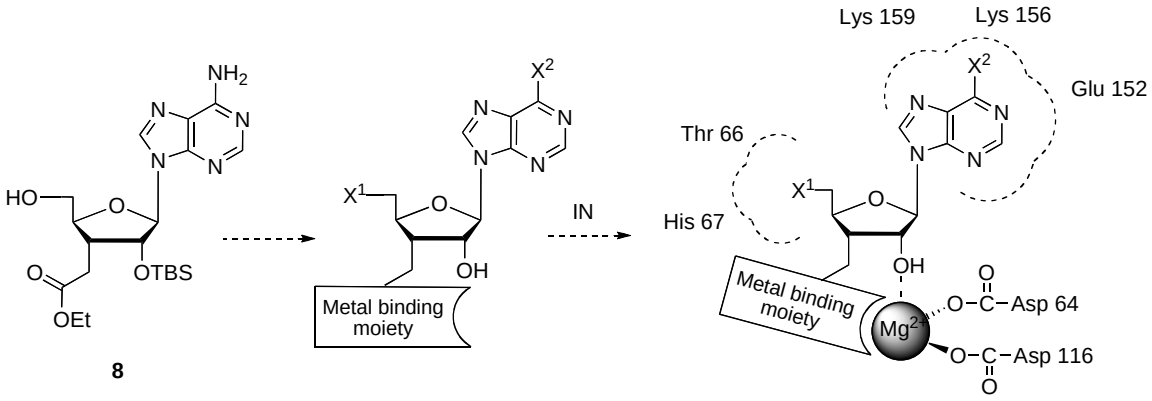

Table 1. Activities of test compounds in biochemical assays

				IC_{50}[d] (μM)	
Compd	ED_{50}[a] (μM)	CT_{50}[b] (μM)	CT_5[c] (μM)	EP[e]	ST[f]
1	>13	37.8	6.2	>10	>10
2	>17	22.6	11.3	>10	>10
3	>34	58.5	23.2	>10	>10
4	>19	21.9	9.3	>10	>10
5	>98	385	143	>10	>10
6	>149	812	162	>10	>10
7	>62	175	21	>10	>10

[a]Inhibitory concentration required to protect MT-2 cells from 50% viral induced cell death.
[b]Cytotoxic concentration required to inhibit cell growth by 50%.
[c]Cytotoxic concentration required to inhibit cell growth by 5%.
[d]Inhibitory concentration required to inhibit IN 3'-end processing (EP) or strand transfer (ST) by 50%.
[e]3'-End processing.
[f]Strand transfer.

The interesting cytotoxicities of compounds **1**–**4** prompted our evaluation of these compounds in the NCI 60 human cancer screen. The NCI 60 human cancer screen is a free service offered by the US National Cancer Institute as a rapid means of screening potential anti-cancer agents as a service to the public. The assay consists of colorimetric

determination of total cell count based on a sulphorhodamine-red protein assay.[11] The screening process is a two-tiered process involving a rapid single dose assay (performed at 10 μM compound concentration), followed by more extensive multi-dose testing. The results for the single dose assay for compounds **1**–**4** are illustrated in Table 2. Compounds **1** and **2** showed promising antiproliferative activities against most of the leukemias, and several other cell lines were also of interest. Importantly, COLO 205 was inhibited by nearly 100% in the single dose assay by compound **2**. Compounds **3** and **4** were much less active, suggesting that perhaps the lactone moiety is saponified to the free carboxylic acid in the assay conditions and may not be able to traverse the cell member to interact with their supposed intracellular target(s). The promising activities of compounds **1**–**2** in the single dose assay assured their candidacy for the multi-dose screen. The results from these assays are shown in Tables 3 and 4.

Compounds **1** and **2** showed low μM inhibition of all six leukemias tested (Tables 3 and 4). A significant number of cell lines from the other subclasses were also inhibited at the low μM level. Compound **2** appeared to be somewhat more toxic than compound **1** toward the leukemia cell lines as evidenced by LC_{50} values for **2** ranging from 9.43–59.0 μM for leukemias SR, HL-60(TB), and RPMI-8226; in contrast to the LC_{50} values for compound **1** which were > 100 μM for all leukemias except RPMI-8226. LC_{50} values for compounds **1** and **2** were identical for leukemia RPMI-8226 (i.e., 59.0 μM). Compound **1** was more toxic than **2** (16 cell lines showed LC_{50} values < 100 μM for **1** while only three cell lines showed the same sensitivity for compound **2**). A majority of cell lines showed LC_{50} values > 100.0 μM for compound **2**. Compound **1** showed greater efficacy in cell growth inhibition than compound **2**. For example, a total of 35 cell lines had GI_{50}

Table 2. Results of Single Dose Growth Inhibition Assay (GI Percent at 10 μM)[a]

Cell Line	1	2	3	4	Cell Line	1	2	3	4
Leukemia					**CNS Cancer**				
CCRF-CEM	50	—	92	94	SF-268	59	33	103	100
HL-60(TB)	45	-33	87	83	SF-295	16	-41	100	103
K-562	59	16	93	81	SF-539	53	0	98	104
MOLT-4	50	-11	85	70	SNB-19	94	37	106	103
RPMI-8226	11	-75	98	105	SNB-75	63	-7	94	97
SR	28	-56	90	90	U251	34	-15	110	96
Non-Small Cell Lung Cancer					**Ovarian Cancer**				
A549/ATCC	22	2	95	120	IGROV1	51	-37	91	92
EKVX	64	21	103	102	OVCAR-3	80	8	95	92
HOP-62	79	60	98	94	OVCAR-4	61	19	106	106
HOP-92	63	-34	87	71	OVCAR-5	100	44	96	97
NCI-H226	76	41	106	99	OVCAR-8	65	20	103	96
NCI-H23	92	48	105	90	SK-OV-3	94	41	106	102
NCI-H322M	91	79	100	101	**Renal Cancer**				
NCI-H460	48	18	112	114	786-0	76	48	105	98
NCI-H522	80	66	107	106	A498	71	46	100	94
Colon Cancer					ACHN	69	12	101	95
COLO 205	43	-100	104	110	CAKI-1	82	43	101	100
HCC-2998	62	-13	106	93	RXF393	-45	-68	-29	-23
HCT-116	17	17	100	98	SN12C	61	17	118	113
HCT-15	56	12	91	92	TK-10	44	7	101	99
HT29	27	-26	109	110	UO-31	57	-7	79	64
KM12	43	17	106	106	**Breast Cancer**				
SW620	71	24	105	106	BT-549	82	26	104	100
Melanoma					HS578T	44	4	111	105
LOX IMVI	50	19	93	63	MCF7	18	3	92	98
MALME-3M	55	12	97	100	MDA-MB-231/ATCC	51	15	123	99
M14	67	34	107	105	MDA-MB-435	54	8	109	102
SK-MEL-2	54	-4	91	70	NCI/ADR-RES	86	54	102	97
SK-MEL-28	84	8	118	107	T-47D	27	-34	103	92
SK-MEL-5	58	26	106	110	**Prostate Cancer**				
UACC-257	88	6	122	125	DU-145	63	25	109	110
UACC-62	80	34	107	99	PC-3	47	-21	97	100

[a]Growth inhibition percent calculated as:
$[(T_i-T_z)/C-T_z)] \times 100$ for $T_i \geq T_z$
$[(T_i-T_z)/T_z)] \times 100$ for $T_i < T_z$
Where T_z = absorbance at t = 0; T_i = absorbance at t = 48 h (10 μM test compound);
C = absorbance of control at t = 48 h

Table 3. Results of Multi-Dose Growth Inhibition Assay for compound **1** (μM)[a]

Cell Line	GI_{50}	TGI	LC_{50}	Cell Line	GI_{50}	TGI	LC_{50}
Leukemia				**CNS Cancer**			
CCRF-CEM	6.69	88.6	>100.0	SF-268	6.53	27.0	92.5
HL-60(TB)	3.01	——	>100.0	SF-295	5.73	>100.0	>100.0
K-562	3.59	32.9	>100.0	SF-539	5.19	>100.0	>100.0
MOLT-4	2.39	23.3	>100.0	SNB-19	29.0	>100.0	>100.0
RPMI-8226	1.09	4.57	59.0	SNB-75	4.56	>100.0	>100.0
SR	2.23	7.07	>100.0	U251	4.69	20.9	76.0
Non-Small Cell Lung Cancer				**Ovarian Cancer**			
A549/ATCC	4.18	19.2	79.1	IGROV1	3.85	18.0	79.2
EKVX	17.7	>100.0	>100.0	OVCAR-3	4.59	17.2	91.3
HOP-62	8.96	26.4	73.1	OVCAR-4	1.23	>100.0	>100.0
HOP-92	<0.01	——	41.2	OVCAR-5	31.1	>100.0	>100.0
NCI-H226	>109	>100.0	>100.0	OVCAR-8	4.92	77.2	>100.0
NCI-H23	33.3	>100.0	>100.0	SK-OV-3	21.0	>100.0	>100.0
NCI-H322M	>100.0	>100.0	>100.0	**Renal Cancer**			
NCI-H460	5.54	2.5.0	>100.0	786-0	2.00	5.21	17.9
NCI-H522	4.36	85.7	>100.0	A498	3.34	17.1	>100.0
Colon Cancer				ACHN	8.55	>100.0	>100.0
COLO 205	3.84	>100.0	>100.0	CAKI-1	29.7	>100.0	>100.0
HCC-2998	>100.0	>100.0	>100.0	RXF393	2.01	4.63	19.5
HCT-116	3.20	16.1	45.6	SN12C	9.10	>100.0	>100.0
HCT-15	8.50	>100.0	>100.0	TK-10	12.4	40.5	>100.0
HT29	4.20	>100.0	>100.0	UO-31	12.1	29.5	71.7
KM12	3.95	20.9	>100.0	**Breast Cancer**			
SW620	4.80	28.4	>100.0	MCF7	3.42	45.1	>100.0
Melanoma				NCI/ADR-RES	>100.0	>100.0	>100.0
LOX IMVI	5.46	>100.0	>100.0	MDA-MB-231/ATCC	3.96	41.3	>100.0
MALME-3M	10.3	>100.0	>100.0	HS578T	3.60	53.6	>100.0
M14	2.51	11.6	7.86	MDA-MB-435	6.21	>100.0	>100.0
SK-MEL-2	5.42	33.1	>100.0	BT-549	>100.0	>100.0	>100.0
SK-MEL-28	6.85	20.2	48.7	T-47D	2.55	>100.0	>100.0
SK-MEL-5	4.34	>100.0	>100.0	**Prostate Cancer**			
UACC-257	5.68	>100.0	>100.0	PC-3	2.25	4.85	12.5
UACC-62	>100.0	>100.0	>100.0	DU-145	4.97	19.4	78.4

[a] GI_{50} = concentration at which cell growth is inhibited by 50%; TGI = concentration required to achieve total growth inhibition; LC_{50} = concentration required to achieve 50% reduction in measured protein after 48 h test period. TGI signifies a cytostatic effec; LC_{50} signifies a cytotoxic effect.

$[(T_i-T_z)/C-T_z)] \times 100 = 50$ for GI_{50}
$T_i = T_z$ for TGI
$[(T_i-T_z)/T_z)] \times 100 = -50$ for LC_{50}

Where T_z = absorbance at t = 0; T_i = absorbance at t = 48 h;
C = absorbance of control at t = 48 h

Table 4. Results of Multi-Dose Growth Inhibition Assay for compound **2** (μM)[a]

Cell Line	GI_{50}	TGI	LC_{50}	Cell Line	GI_{50}	TGI	LC_{50}
Leukemia				**CNS Cancer**			
CCRF-CEM	6.37	>100.0	>100.0	SF-268	8.29	>100.0	>100.0
HL-60(TB)	1.81	4.34	16.4	SF-295	9.09	>100.0	>100.0
K-562	3.12	>100.0	>100.0	SF-539	22.3	>100.0	>100.0
MOLT-4	2.23	2.23	>100.0	SNB-19	>100.0	>100.0	>100.0
RPMI-8226	1.58	1.58	59.0	SNB-75	12.7	>100.0	>100.0
SR	1.27	1.27	9.43	U251	5.66	>100.0	>100.0
Non-Small Cell Lung Cancer				**Ovarian Cancer**			
A549/ATCC	9.35	>100.0	>100.0	IGROV1	3.72	65.7	>100.0
EKVX	26.4	>100.0	>100.0	OVCAR-3	7.11	>100.0	>100.0
HOP-62	24.9	>100.0	>100.0	OVCAR-4	53.0	>100.0	>100.0
HOP-92	2.71	24.3	>100.0	OVCAR-5	38.2	>100.0	>100.0
NCI-H226	41.9	>100.0	>100.0	OVCAR-8	9.02	>100.0	>100.0
NCI-H23	>100.0	>100.0	>100.0	SK-OV-3	52.7	>100.0	>100.0
NCI-H322M	>100.0	>100.0	>100.0	**Renal Cancer**			
NCI-H460	7.49	>100.0	>100.0	786-0	9.01	>100.0	>100.0
NCI-H522	11.1	>100.0	>100.0	A498	3.87	40.3	>100.0
Colon Cancer				ACHN	14.4	>100.0	>100.0
COLO 205	12.3	>100.0	>100.0	CAKI-1	53.8	>100.0	>100.0
HCC-2998	30.6	>100.0	>100.0	RXF393	9.74	38.0	>100.0
HCT-116	4.20	>100.0	>100.0	SN12C	85.3	>100.0	>100.0
HCT-15	6.47	>100.0	>100.0	TK-10	20.5	>100.0	>100.0
HT29	5.37	>100.0	>100.0	UO-31	7.79	>100.0	>100.0
KM12	23.9	>100.0	>100.0	**Breast Cancer**			
SW620	>100.0	>100.0	>100.0	MCF7	5.59	>100.0	>100.0
Melanoma				NCI/ADR-RES	>100.0	>100.0	>100.0
LOX IMVI	7.30	>100.0	>100.0	MDA-MB-231/ATCC	12.3	>100.0	>100.0
MALME-3M	14.1	>100.0	>100.0	HS578T	5.79	>100.0	>100.0
M14	15.2	>100.0	>100.0	MDA-MB-435	10.9	>100.0	>100.0
SK-MEL-2	14.9	83.1	>100.0	BT-549	29.0	>100.0	>100.0
SK-MEL-28	7.77	>100.0	>100.0	T-47D	13.9	>100.0	>100.0
SK-MEL-5	5.81	>100.0	>100.0	**Prostate Cancer**			
UACC-257	22.6	>100.0	>100.0	PC-3	___	___	___
UACC-62	41.9	>100.0	>100.0	DU-145	1.66	>100.0	>100.0

[a] GI_{50} = concentration at which cell growth is inhibited by 50%; TGI = concentration required to achieve total growth inhibition; LC_{50} = concentration required to achieve 50% reduction in measured protein after 48 h test period. TGI signifies a cytostatic effec; LC_{50} signifies a cytotoxic effect.

$[(T_i-T_z)/C-T_z)] \times 100 = 50$ for GI_{50}
$T_i = T_z$ for TGI
$[(T_i-T_z)/T_z)] \times 100 = -50$ for LC_{50}

Where T_z = absorbance at t = 0; T_i = absorbance at t = 48 h;
C = absorbance of control at t = 48 h

values ≤ 6 μM for **1**, whereas only 14 cell lines were inhibited at similar levels for compound **2**.

A COMPARE[12] analysis of the GI_{50} data for compound **1** suggested that protein kinases might be molecular targets for this type of compound. Kinases for which there was significant correlation between kinase expression and cytotoxicity of compound **1** included EGFR, ERBB2, ERBB3, PTK2, and PTK6, each of which has been implicated in cancer.

To verify actual binding of compound **1** to cancer- and other disease-related protein kinases, compound **1** was screened against a commercially available panel of protein kinases (KinomeScan™, Ambit Biosciences).[13] The KinomeScan™ assay is a competitive binding assay based on phage-display of protein kinases and immobilized ATP-binding site ligands.[14] Binding of protein kinases expressed on the surface of bacteriaphage T7 to immobilized ATP-binding site ligands was inhibited by compound **1** for 11 of the 353 protein kinases evaluated.[15] Binding inhibition for these 11 kinases was ≥ 30% while a majority of the kinases were unaffected by **1** showing binding inhibitions of ≤ 10% (Figure 7).

Figure 7. Inhibition of binding of protein kinases to ATP-binding site ligands by **1**.

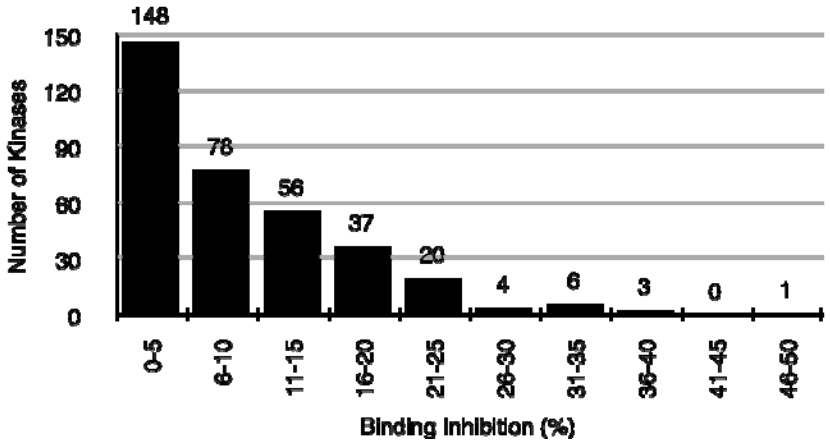

Selective inhibition of protein kinases is a desirable property and suggests that compound **1** and/or derivatives may have considerable potential in therapeutic applications.[16] Kinases for which binding was inhibited by ≥ 30% included EGFR, TYK2, FLT3, CSNK2A2, PAK3, MARK3, BTK, IKK-α, CSNK1G2, RPS6KA1, and BMPR1B, each of which has been implicated in various forms of cancer (Figure 8).

Figure 8. Binding inhibition ≥ 30% observed in 11 of 353 protein kinases.

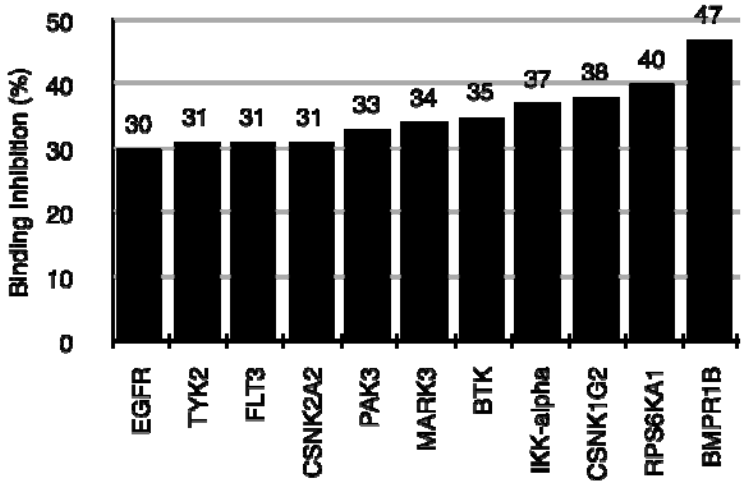

Binding inhibition was greatest for BMPR1B (or ALK6), a protein kinase recently implicated in estrogen receptor positive breast cancer. [17] The relatively pronounced inhibition of binding of ALK6 compared to other members of the ALK family of protein kinases suggests that **1** might be a useful probe for elucidating the role played by ALK6 in BMP-mediated signaling (Figure 9). [18] Selective inhibition of binding was also observed for other protein kinase families (e.g.; p38 and PAK kinase families, Figures 10 and 11).

Figure 9. Selective inhibition binding of Alk6 by compound **1**.

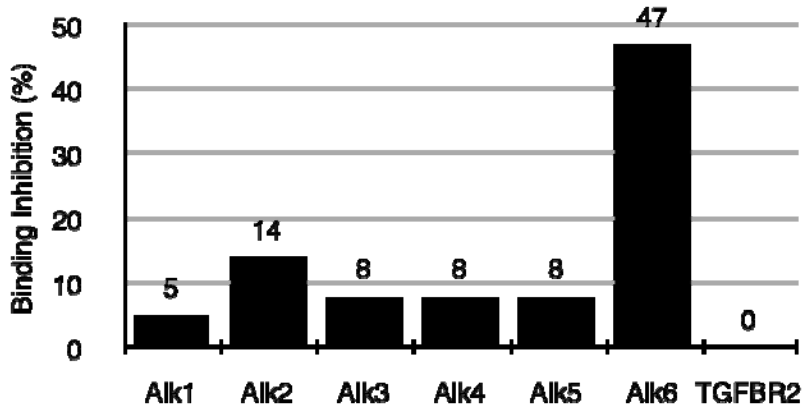

Figure 10. Selective inhibition of binding to p38 protein kinases by compound **1**.

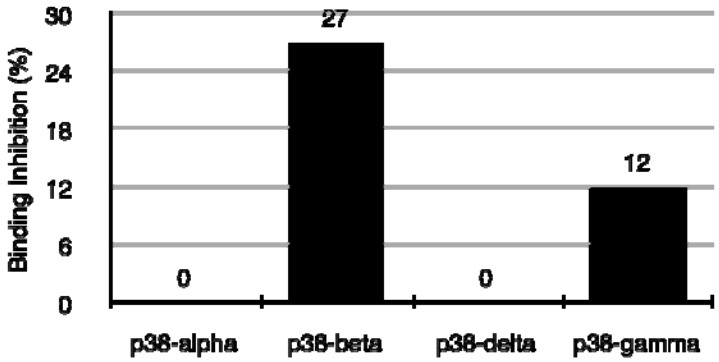

Figure 11. Selective inhibition of binding to PAK protein kinases by compound **1**.

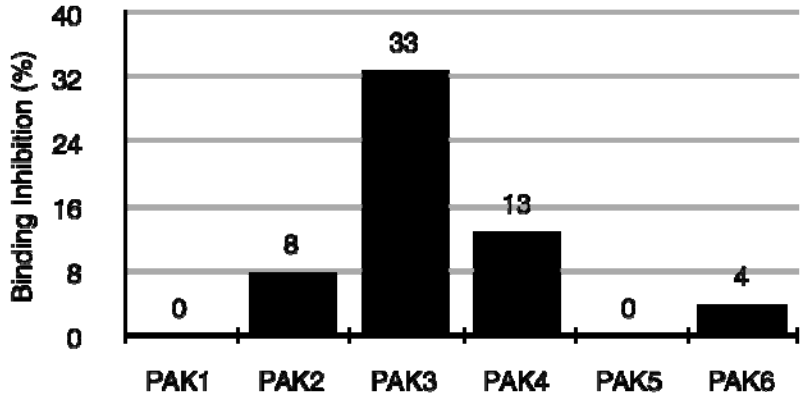

Compound **1** was also screened for its ability to inhibit a panel of cancer-related protein kinases (Figure 12). Activities for several of the protein kinases were modestly enhanced at 20 μM compound concentration and two of the kinases (FMS and PAK4) were inhibited. The assay employed was based on inhibition of phosphorylation of an unnatural protein substrate in the presence of radio-labeled ATP. While this assay has been validated as a means of discovering protein kinase inhibitors in vitro, the relevance of the results obtained with an unnatural protein substrate remains somewhat in question. The modest inhibition of PAK4 and FMS in vitro therefore may not be particularly relevant in a biological context.

Figure 12. Inhibition of cancer-related protein kinases by compound **1** (20 μM).

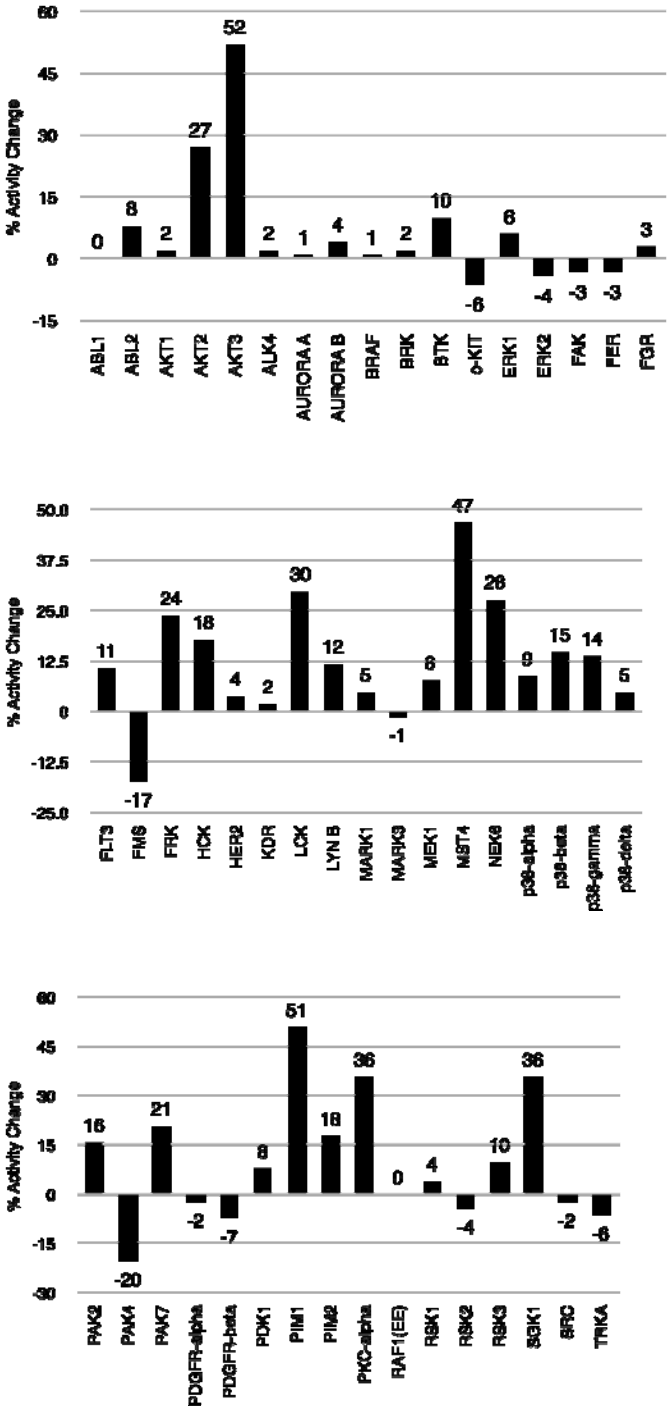

Results and Discussion

In order to explore the structural features required for anti-proliferative activity, we sought to prepare a series of compounds that would probe the importance of substituents in the SE and SW quadrants of compound **1** (Figure 13).

Figure 13. Quadrants for SAR of compound **1**.

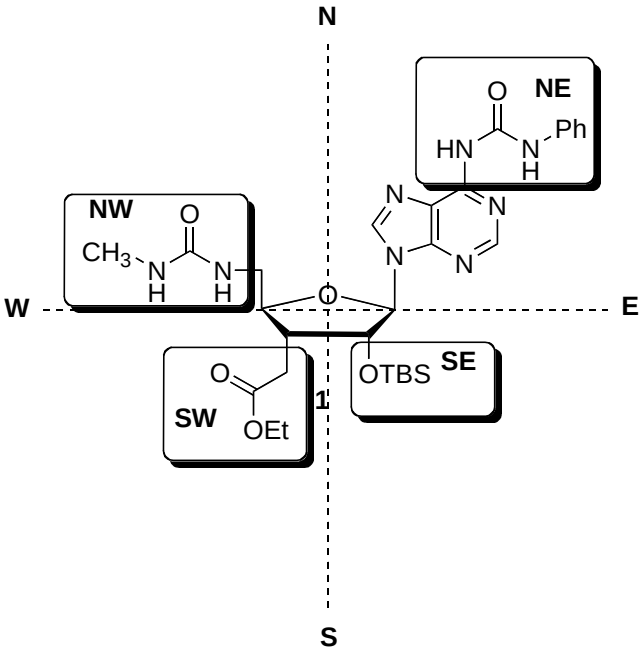

Based on the assumption that compound **1** exerts its effect as an ATP-binding site competitive inhibitor, we assumed for this initial Structure Activity Relationship Study (SAR) that substituents in the NE and NW quadrants are necessary for binding in the hydrophobic pocket and phosphate binding pockets, respectively (see ATP binding site pharmacophore model in Figure 2). The relatively poor anti-proliferative activities of compounds **3** and **4** suggested that the bulky 2′-O-TBS group is necessary for activity. However, the lability of the lactone moieties possessed by **3** and **4** (i.e. susceptibility to saponification and/or acylation by endogenous amines) did not preclude other reasons for the poor anti-proliferative activity, namely poor bioavailability caused by saponification to the carboxylic acid or reaction with nucleophilic amino acid side chains.

Saponification of the lactone moiety would yield a negatively charged carboxylate that would not be expected to diffuse across the cell membrane, and acylation of basic amino acid side chains such as lysine might result in a significant decrease in intracellular concentration of **3** and **4** via covalent linkage to "by-stander" proteins. Both of these mechanisms could account for the lack of activity exhibited by compounds **3** and **4**. In order to test whether the lack of activity exhibited by **3** and **4** was due to one of these mechanisms, or perhaps due to their lack of a bulky substituent at the 2′ position, compounds **9**–**11** were chosen as synthetic targets (Figure 14).

Figure 14. Targets for structure activity study (SAR)

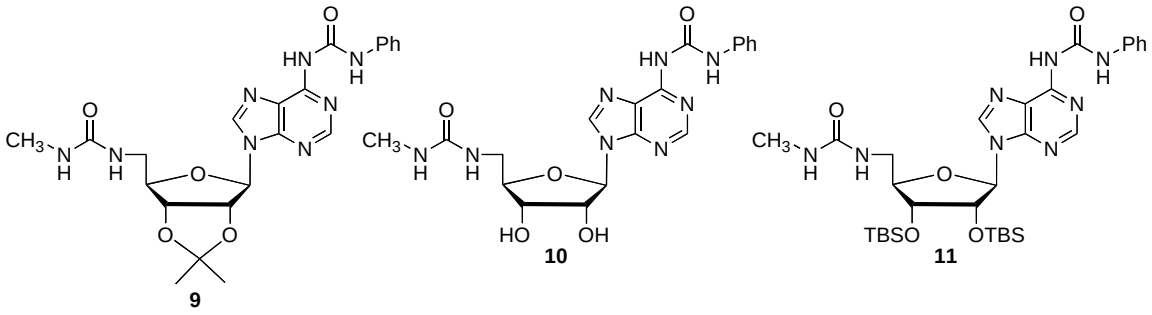

The synthetic approach to compounds **9**–**11** is illustrated in Schemes 1 and 2, respectively. The synthesis of compounds **9**–**11** began with compound **12** which was prepared via a literature procedure. Treatment of compound **12** with phenylisocyanate in anhydrous CH_2Cl_2 for 5 days gave compound **13** in 87% isolated yield. It was found that diphenylurea is formed as a byproduct in this reaction (via hydrolysis of phenylisocyanate from adventitious water), and that the complex between the diphenylurea byproduct and compound **13** was almost completely insoluble in most common chromatography solvents.

Scheme 1. Synthesis of compound **9** and **10**.

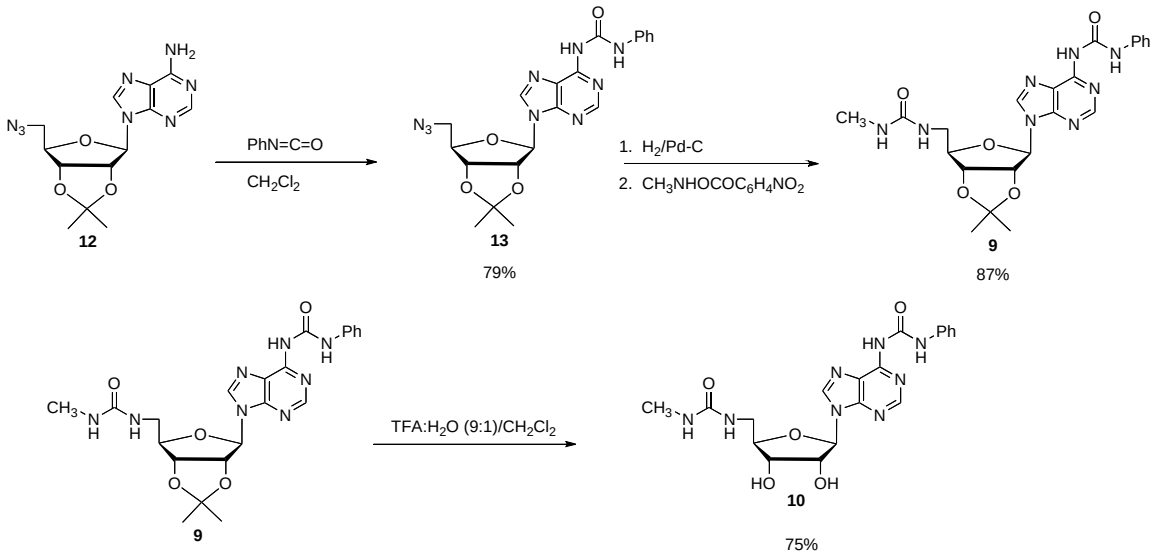

Scheme 2. Synthesis of compound **11**.

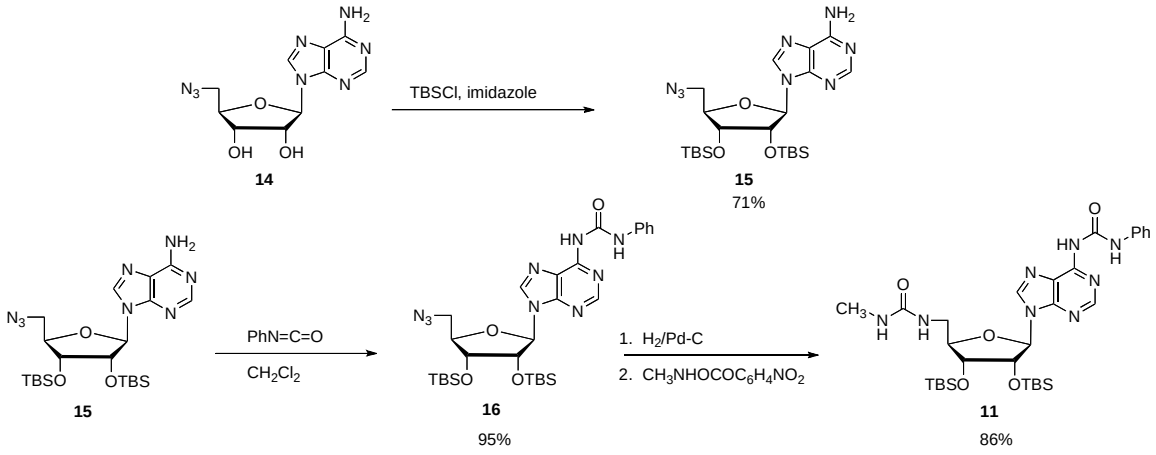

The diphenylurea byproduct formed even when compound **12** was dried under vacuum or via azeotropic removal of water by evaporation of benzene. Removal of the reaction solvents prior to chromatography also seemed to give larger amounts of the diphenylurea byproduct and complicated getting the crude reaction material back into solution in order to be able to apply it to the chromatography column. We found that simply running the reaction at rather high dilution and then direct addition of the reaction mixture to a chromatography column avoided the problem of complex formation between diphenylurea and compound **13**. The highest yields were obtained for compound **13** when this procedure was followed.

Compound **13** was converted to compound **9** in 87% yield via a one-pot tandem reduction of the azide followed by acylation of the resulting amine intermediate with *p*-nitrophenyl N-methylcarbamate. *p*-Nitrophenyl N-methylcarbamate is a safe and easy-to- handle alternative to the more dangerous reagent methylisocyanate.[19] Compound **9** was converted to compound 10 via TFA-promoted (trifluoracetic acid) hydrolysis of the acetal. Chromatography using an EtOAc/iPrOH/H_2O mixture (4:2:1) gave compound **10** in 75% yield.

Compound **11** was prepared from compound **14** via a three-step procedure. Silylation of compound **14** to give **15** was accomplished by treating 14 with TBSCl (3 equiv) and imidazole (excess). Application of this method to the preparation of **15** gave desired product in 71% yield. Conversion of **15** to **11** was accomplished using reagents and conditions similar to those used to prepare compound **9** from compound **12**. Compound **16** and diphenylurea had nearly identical R_fs in EtOAc/hexanes solvents, but good separation (by TLC) could be achieved using neat CH_2Cl_2. Flash chromatography of **16** using 4 column lengths of neat CH_2Cl_2 followed by EtOAc/Hexanes (3:7) gave product

which was mostly pure of the diphenylurea. However, residual "TLC-visible" quantities could be seen in the purified material. Fortunately, diphenylurea byproduct was easily separated out at the next step since it has a significantly higher R_f than compound **11**.

Compounds **9** and **10** were submitted to the NCI for screening against the NCI 60. Interestingly, compounds **9** and **10** had very little anti-proliferative activity at 10 μM compound concentration (Table 5). This result strongly suggests that the bulky 2′-*O*-TBS group is necessary for optimum anti-proliferative activity.

To further probe structural features that might lead to anti-cancer activity, compounds from the chemical inventory in the Peterson group were submitted for screening (Figure 15). The results from these assays are illustrated in the Appendix. It is interesting to note that from this SAR it appears that the following substitution patterns are necessary for optimal anti-proliferative activity: (1) N-phenylurea in the NE quadrant; (2) N-methyl-urea or –urethane in the NW quadrant; (3) *O*-TBS substitution in the SE quadrant. Substitution in the SW was also evaluated and results from the NCI screening of compound **11** shed important light on the importance of a bulky 3′-*O*-TBS. Importantly, such substitution did not abrogate the anti-proliferative activities imparted by the NE, NW, and SE substitutions. Compound **11** is significantly easier to prepare than either compounds **1** or **2** and provides a synthetically versatile template for more in-depth SAR studies. Synthetic targets for this study are illustrated in Scheme 3. Discussion of the synthesis of this library of compounds follows.

Table 5. Single Dose Growth Inhibition Assay for **9** and **10** (GI Percent at 10 μM)[a]

Cell Line	**9**	**10**	Cell Line	**9**	**10**
Leukemia			**CNS Cancer**		
CCRF-CEM	95	100	SF-268	91	99
HL-60(TB)	84	79	SF-295	119	123
K-562	90	60	SF-539	84	91
MOLT-4	103	—	SNB-19	85	89
RPMI-8226	87	90	SNB-75	60	66
			U251	94	86
Non-Small Cell Lung Cancer			**Ovarian Cancer**		
A549/ATCC	103	99	OVCAR-3	89	85
EKVX	102	113	OVCAR-4	90	92
HOP-62	99	96	OVCAR-5	109	102
HOP-92	14	71	OVCAR-8	100	105
NCI-H226	109	99	SK-OV-3	79	77
NCI-H23	87	95			
NCI-H322M	101	95	**Renal Cancer**		
NCI-H460	101	101	786-0	105	106
NCI-H522	104	92	A498	87	103
			ACHN	105	99
Colon Cancer			CAKI-1	73	55
HCC-2998	96	78	RXF393	97	114
HCT-116	81	89	SN12C	95	96
HCT-15	98	—	TK-10	134	152
HT29	99	97	UO-31	74	98
KM12	90	89	**Breast Cancer**		
SW620	91	98	BT-549	72	—
			HS578T	102	93
Melanoma			MCF7	85	91
LOX IMVI	100	99	MDA-MB-231/ATCC	107	90
MALME-3M	76	97	MDA-MB-468	100	98
M14	89	108	T-47D	75	78
SK-MEL-2	104	117			
SK-MEL-28	92	100	**Prostate Cancer**		
SK-MEL-5	86	94	DU-145	94	95
UACC-257	107	105	PC-3	71	85
UACC-62	92	88			

[a]Growth inhibition percent calculated as:
$[(T_i-T_z)/C-T_z)]$ X 100 for $T_i \geq T_z$
$[(T_i-T_z)/T_z)]$ X 100 for $T_i < T_z$
Where T_z = absorbance at t = 0; T_i = absorbance at t = 48 h (10 μM test compound);
C = absorbance of control at t = 48 h

Figure 15. Structures of inventory compounds.

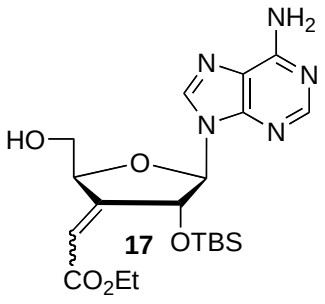

NSC: 749605

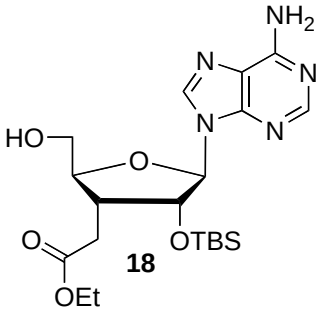

NSC: 749604

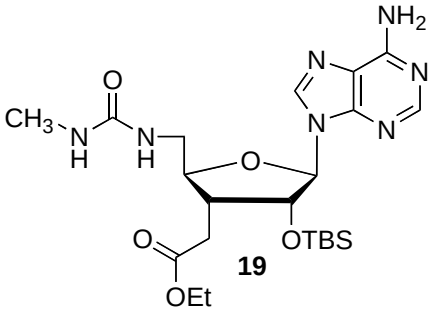

NSC: 749602

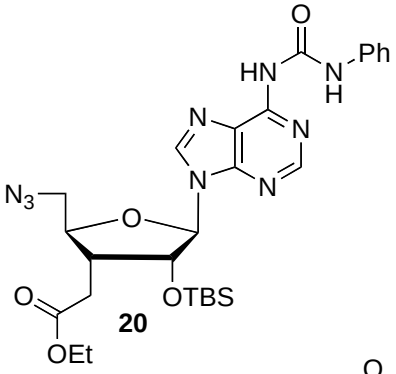

NSC: 749603

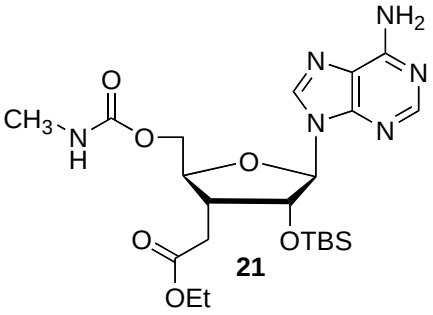

NSC: 749601

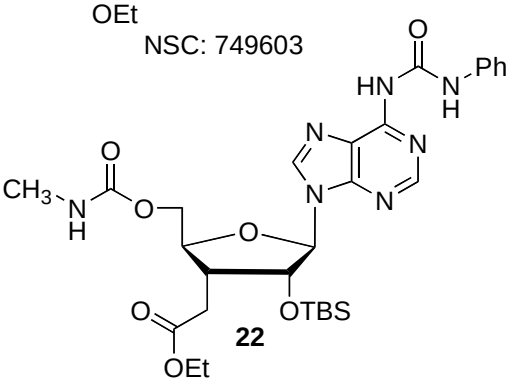

NSC: 749600

Scheme 3. Synthetic targets for more in-depth SAR.

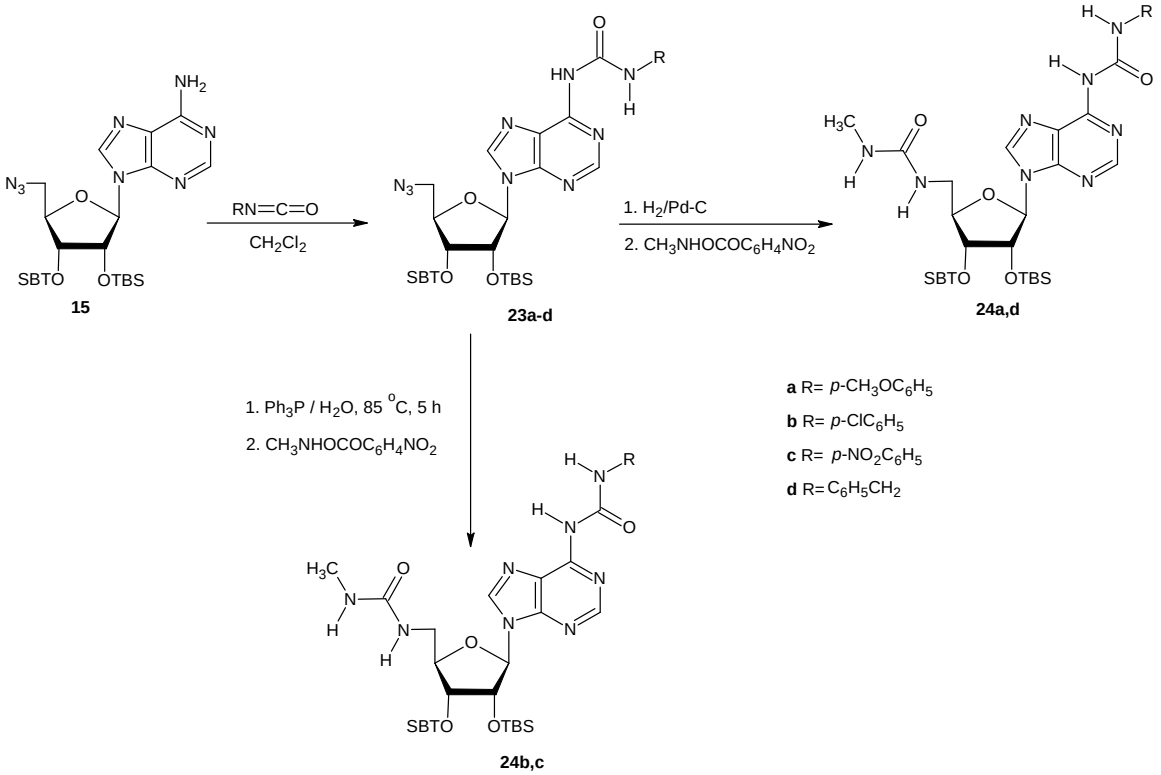

Compounds **23a**–**d** were prepared by treating **15** with the appropriate isocyanate in dilute CH_2Cl_2 solution. The reactions generally required 5 days at ambient temperature. Work-up for **23a**–**d** was similar to that for compound **16** and could be achieved by simple chromatography of the crude reaction mixture to give **23a**–**d** in good yields. Reduction of the azide using standard hydrogenation conditions (H_2/Pd-C) proved problematic for **23b**,**c** as these compounds have moieties which are susceptible to hydrogenolysis. Successful reduction of the azide was achieved by Staudinger reduction conditions (Ph_3P followed by H_2O) which afforded the desired products (**24b**,**c**) in acceptable yields. Compounds **24a**–**d** are currently being screened for antiproliferative activity and that data will be published as soon as it is available.

Conclusion

A series of N^6,5′-bis-ureidoadenosine derivatives was prepared and tested for activities in antiproliferative assays against the NCI 60 panel of human cancers. From this study it is concluded that a 2′-*O*-TBS group is necessary (but not sufficient) for growth inhibition, as is also true for the 5′- and N^6-ureido substitutions. When occurring individually in the absence of the other, neither 5′- nor N^6-ureido or N^6-carbamoyl substitution gave rise to potent growth inhibition, even in the presence of the essential 2′-*O*-TBS moiety, as evidenced by the almost complete lack of activity for compounds **17**–**21** (Figure 15 and Appendix). Substitution of a carbamoyl group for the urea in the NW quadrant gave compound **22** which also exhibited comparable activities to compound **1**. Very recently obtained data suggests that the synthetically-more-accessible compound **11** may exhibit activities comparable to the more challenging lead compound **1** (see Appendix for single-dose antiproliferative data for compound **11**; NSC 750689). Compound **11** offers a synthetically viable alternative for preparing more extensive compound libraries based on the easier-to-prepare bis-*O*-TBS-substituted adenosine template (e.g. compounds **24a**–**d**). We are currently pursuing this line of research and results from such studies will be reported shortly.

Experimental Section

General Experimental

Flash chromatography was carried out using 230–400 mesh silica gel. Preparative TLC was performed using Merck Kieselgel 60 F_{254} sheets. UV spectra were obtained in MeOH and water. ^{1}H NMR spectra were obtained on either a Varian 300 MHz or a Varian 500 MHz spectrometer using internal references at δ 7.27 ($CDCl_3$) and δ 2.50 (DMSO-d_6). ^{13}C NMR spectra were obtained using internal references at δ 77.3 ($CDCl_3$) and δ 39.5 (DMSO-d_6). High resolution mass spectra were obtained by using FAB and ESI techniques. Commercially available reagents were used as supplied. All water sensitive reactions were performed in flame-dried flasks under Nitrogen or Argon. Solvents used in the reactions were dried by passing through columns of activated alumina under Argon.

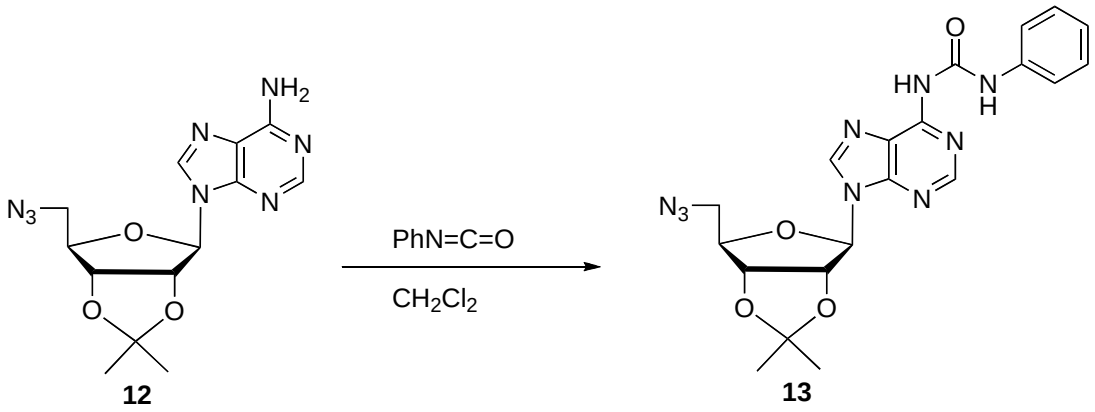

12 **13**

5'-azido-5'-deoxy-2', 3'-*O*-isopropylidene-N^6-(*N*-phenylcarbamoyl)adenosine (13).

To a flame dried flask containing compound **12** (454 mg, 1.37 mmol) was added phenylisocyanate (190 mg, 1.6 mmol) in CH_2Cl_2 (16 mL). The resulting solution was stirred protected from moisture until TLC indicated that starting material had been consumed (5 d). The crude solution was added directly to a flash chromatography column and eluted (50→75%EtOAc/hexanes→10%MeOH/EtOAc). Appropriate fractions were pooled and volatiles were evaporated under reduced pressure to give 5'-azido-5'-deoxy-2', 3'-*O*-isopropylidene-N^6-(*N*-phenylcarbamoyl)adenosine (491 mg, 79%): ^{1}H NMR ($CDCl_3$, 500 MHz) δ 11.71 (s, 1H), 8.66 (s, 1H), 8.25 (s, 1H), 8.21 (s, 1H), 7.66 (d, J = 8.5 Hz, 2H), 7.39 (t, J = 8.0 Hz, 2H), 7.15 (t, J = 7.3 Hz, 1H), 6.19 (d, J = 2.5 Hz, 1H), 5.44 (dd, J = 6.3, 2.3 Hz, 1H), 5.07 (dd, J = 6.0, 3.5 Hz, 1H), 4.43 (dd, J = 9.0, 5.0 Hz, 1H), 3.63 (dd, J = 9.5, 4.8 Hz, 2H), 1.65 (s, 3H), 1.42 (s, 3H); ^{13}C NMR ($CDCl_3$, 125 MHz) δ 151.2, 151.1, 150.2, 149.9, 142.1, 137.9, 129.1, 124.1, 121.1, 120.4, 115.1, 90.7, 85.3, 84.1, 81.8, 52.3, 27.2, 25.4; MS (FAB) *m/z* 452.17923 (MH^+ $[C_{20}H_{22}N_9O_4]$ = 452.17948).

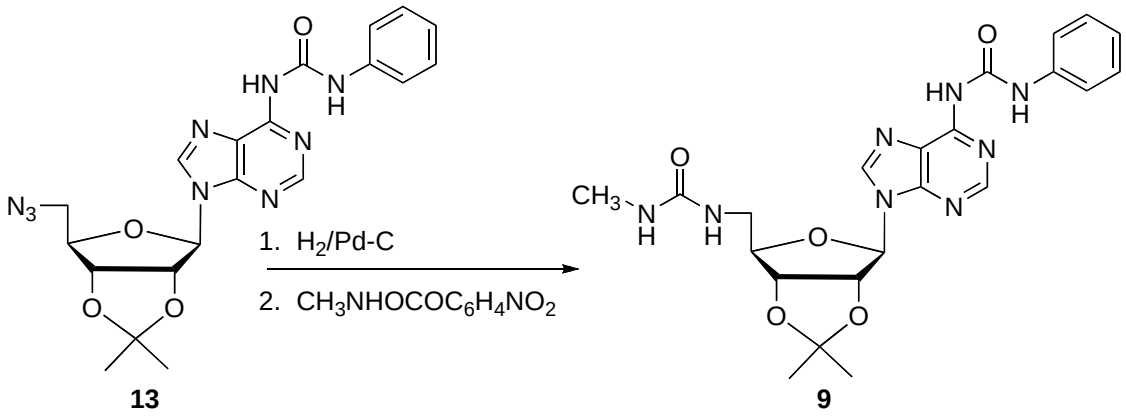

13 9

5'-Deoxy-2', 3'-*O*-isopropylidene-5'-[(*N*-methylcarbamoyl)amino]-N^6-(*N*-phenylcarbamoyl)adenosine (9).

A solution of **13** (70 mg, 0.16 mmol) and 10% Pd–C (40 mg) in EtOAc (10 mL) was vigorously stirred for 15 h under an atmosphere of H_2 (balloon pressures). *p*-Nitrophenyl *N*-methylcarbamate (43 mg, 0.22 mmol) and anhydrous Na_2CO_3 (45 mg, 0.43 mmol) were added, and the resulting mixture was stirred for 4 h under N_2. Solids were removed via filtration (celite/EtOAc →MeOH), and volatiles were evaporated under reduced pressure. The crude residue was chromatographed (5→10% MeOH/CH_2Cl_2) to give **9** (65 mg, 87%): ^{1}H NMR ($CDCl_3$, 500 MHz) δ 12.10 (s, 1H), 9.79 (s, 1H), 8.69 (s, 1H), 8.68 (s, 1H), 7.56 (dd, *J* = 8.8, 0.8 Hz, 2H), 7.40 (t, *J* = 8.0 Hz, 2H), 7.20 (t, *J* = 8.0 Hz, 1H), 6.15 (d, J = 4.0 Hz, 1H), 5.84 (m, 1H), 5.27 (dd, *J* = 6.3, 3.8 Hz, 1H), 4.98 (dd, *J* = 6.3, 2.3 Hz, 1H), 4.77 (m, 1H), 4.52 (dd, *J* = 6.8, 2.8 Hz, 1H), 3.74 (ddd, *J* = 13.8, 7.4, 4.1 Hz, 1H), 3.38 (dt, *J* = 3.8, 14.8 Hz, 1H), 2.56 (d, *J* = 4.5 Hz, 3H), 1.65 (s, 3H), 1.40 (s, 3H); ^{13}C NMR ($CDCl_3$, 125 MHz) δ 159.2, 152.6, 150.9, 150.34, 150.30, 143.3, 137.2, 129.2, 124.9, 121.5, 121.2, 114.6, 91.6, 85.9, 83.9, 81.6, 41.8, 27.4, 26.9, 25.4 ; MS (FAB) *m/z* 483.2099 (MH^+ [$C_{22}H_{27}N_8O_5$] = 483.2099).

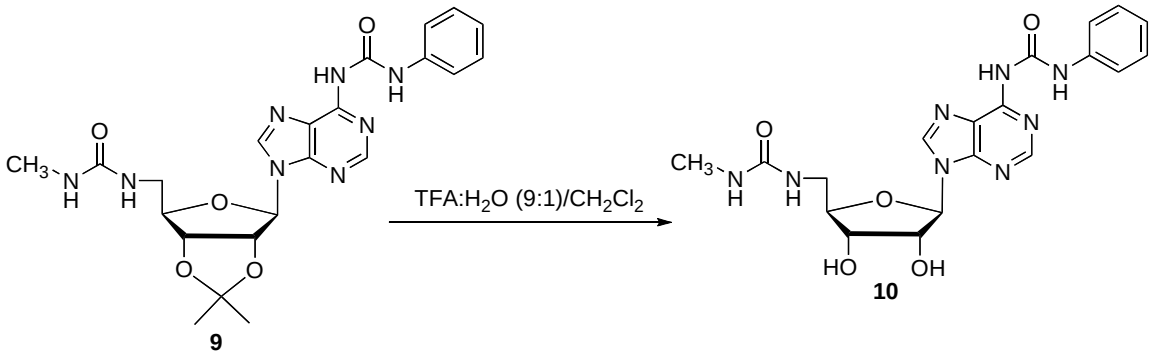

5'-Deoxy-5'-[(*N*-methylcarbamoyl)amino]-N^6-(*N*-phenylcarbamoyl)adenosine (10).

A solution of **9** (10 mg, 0.021 mmol), TFA (100 μL), and H_2O (25 μL) in CH_2Cl_2 (500 μL) was vigorously stirred at ambient temperature until TLC indicated complete conversion to baseline product (4 h). Volatiles were removed under reduced pressure (≤ 25 °C) and the crude was purified via flash chromatography (EtOAc/iPrOH/H_2O) to give **10** (7 mg, 75%): ^{1}H NMR ($CDCl_3$, 500 MHz) δ 11.75 (s, 1H), 10.21 (s, 1H), 8.71 (s, 1H), 8.70 (s, 1H), 7.61 (d, *J* = 7.5 Hz, 2H), 7.35 (t, *J* = 7.8 Hz, 2H), 7.08 (t, *J* = 7.5 Hz, 1H), 6.10 (s, 1H), 5.97 (d, *J* = 6.0 Hz, 1H), 5.80 (s, 1H), 4.67 (t, *J* = 5.5 Hz, 1H), 4.09 (dd, *J* = 3.5, 5.0 Hz, 1H), 3.94–3.91 (m, 1H), 3.41 (dd, *J* = 14.3, 4.3 Hz, 1H), 3.26 (dd, *J* = 14.3, 6.3 Hz, 1H), 2.49 (s, 3H; overlaps with DMSO); ^{13}C NMR ($CDCl_3$, 125 MHz) δ 159.1, 151.4, 151.2, 151.1, 150.2, 143.4, 138.9, 129.4, 123.7, 121.1, 119.9, 87.9, 84.9, 73.6, 71.6, 42.2, 26.8; MS (FAB) *m/z* 443.17757 (MH^+ [$C_{19}H_{23}N_8O_5$] = 443.17859).

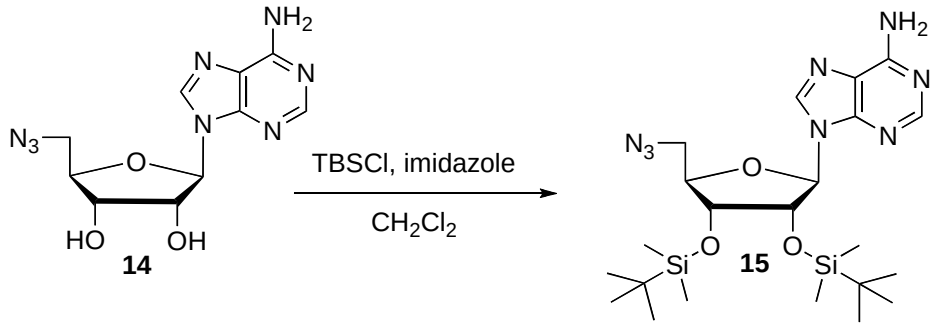

5´-Azido-2´,3´-bis-*O*-*tert*-butyldimethylsilyl-5´-deoxyadenosine (15).

A solution of **14** (50 mg, 0.17 mmol), TBSCl (77 mg, 0.51 mmol), and imidazole (93 mg, 1.4 mmol) in dry DMF (0.25 mL) was stirred at ambient temperature and protected from moisture for 2 days. The crude reaction mixture was added directly to a flash column and eluted using 50% ethyl acetate/hexanes (2 columns), and 75% ethyl acetate/hexanes (3 columns) as eluents. Appropriate fractions were evaporated and the solvents were removed under reduced pressure. Recrystallization from benzene gave **15** (64 mg, 72.1%). ^{1}H NMR ($CDCl_3$, 300 MHz) δ 8.36 (s, 1H), 8.03 (s,1H), 6.20 (s, 2H), 5.91 (d, J = 4.5 Hz, 1H), 4.96 (t, J = 4.4 Hz, 1H), 4.35 (t, J = 4.5 Hz, 1H), 4.22 (dd, J = 9.3, 4.8 Hz, 1H), 3.74 (d, J = 8.0 Hz, 1H), 0.95 (s, 9H), 0.85 (s, 9H), 0.14 (s, 3H), 0.13 (s, 3H), 0.00 (s, 3H), -0.15 (s, 3H); ^{13}C NMR ($CDCl_3$, 75 MHz) δ 156.0, 153.1, 149.7, 140.2, 120.7, 90.0, 83.1, 74.4, 72.6, 51.8, 25.98, 25.88, 18.22, 18.06, -4.23, -4.53, -4.68, -4.75; MS 521.2851 (ES) m/z ($[M+H]^+$ $[C_{22}H_{41}N_8O_3Si_2]$ = 521.2835).

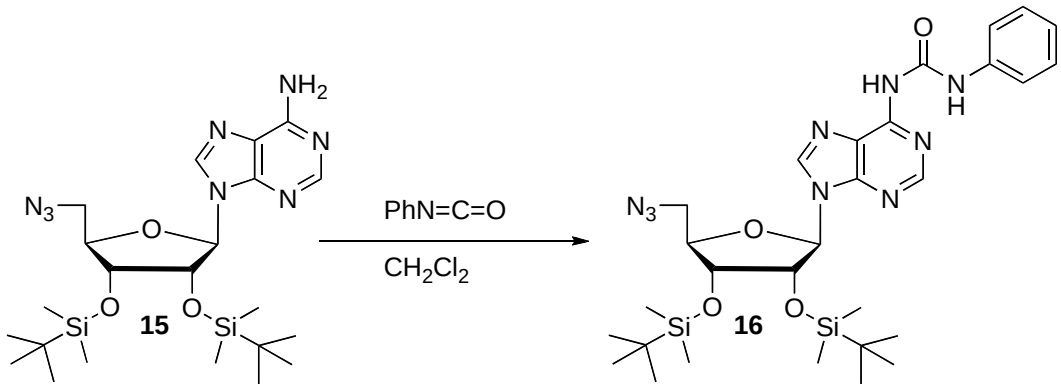

5´-Azido-2´,3´-bis-*O*-*tert*-butyldimethylsilyl-5´-deoxy-N^6-(*N*-phenylcarbamoyl)-adenosine (16).

A solution of compound **15** (125 mg, 0.240 mmol) and phenylisocyanate (0.29 mmol) in CH_2Cl_2 (2.9 mL) was stirred at ambient temperature until TLC indicated complete consumption of starting material (5 days). The crude reaction mixture was added directly to a flash chromatography column and eluted with 20→30% EtOAc/hexanes to give **16** (130 mg, 85%). ^{1}H NMR ($CDCl_3$, 500 MHz) δ 11.78 (s, 1H), 8.61 (s, 1H), 8.46 (bs, 1H), 8.33 (bs, 1H), 7.63 (d, J = 7.5 Hz, 2H), 7.35 (t, J = 7.8 Hz, 2H), 7.11 (t, J = 7.3 Hz, 1H), 5.97 (d, J = 4.0 Hz, 1 H), 4.84 (t, J = 4.5 Hz, 1H), 4.30 (t, J = 4.3 Hz, 1H), 4.22 (t, J = 4.5 Hz, 1H), 3.70 (dd, J = 6.3, 4.8 Hz, 2H), 0.92 (s, 9H), 0.82 (s, 9H), 0.11 (s, 3H), 0.09 (s, 3H), 0.00 (s, 3H), –0.17 (s, 3H); ^{13}C NMR ($CDCl_3$, 125 MHz) δ 151.3, 150.8, 150.1, 142.5, 138.0, 129.0, 123.9, 121.2, 120.4, 89.7, 82.9, 74.7, 72.3, 51.6, 25.8, 25.7, 18.0, 17.9, –4.38, –4.68, –4.84, –4.88; MS (FAB) *m/z* 640.3204 (MH^+ [$C_{29}H_{45}N_9O_4Si_2$]) = 640.3206.

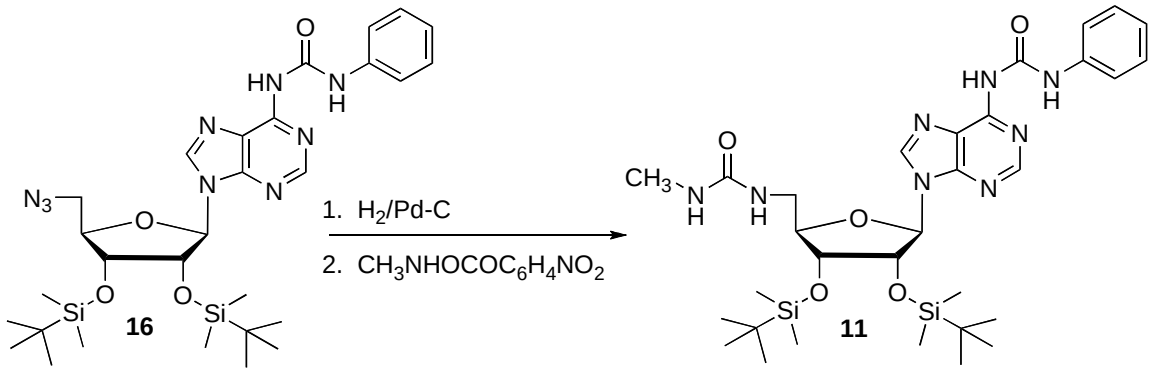

2´,3´-Bis-*O*-*tert*-butyldimethylsilyl-5´-deoxy-5´-(*N*-methylcarbamoyl)amino-N^6-(*N*-phenylcarbamoyl)adenosine (11).

A solution of **16** (123 mg, 0.192 mmol) and 10% Pd-C (50 mg) in EtOAc (10 mL) was stirred overnight under an atmosphere of H_2 (balloon pressures). The mixture was filtered (celite) and volatiles were evaporated. The crude material was dissolved in CH_2Cl_2 (4 mL) and *p*-nitrophenyl-*N*-methyl-carbamate (45 mg, 0.229 mmol) and Et_3N (60 μL, 0.60 mmol) were then added. The mixture was stirred at ambient temperature until TLC showed reaction was complete (9 h). The crude mixture was added to a flash chromatography column and eluted with 75% EtOAc/hexanes → 5% MeOH/EtOAc to give **11** (111 mg, 86%). ^{1}H NMR ($CDCl_3$, 500 MHz) δ 11.92 (bs, 1H), 9.03 (bs, 1H), 8.67 (s, 1H), 8.61 (s, 1H), 7.57 (d, J = 7.5 Hz), 7.39 (t, J = 8.3 Hz, 2H), 7.18 (t, J = 7.3 Hz, 1H), 6.51 (d, J = 6.0 Hz, 1 H), 6.01 (d, J = 8.0 Hz, 1H), 4.74–4.73 (m, 1H), 4.64 (dd, J = 7.5, 4.5 Hz, 1 H), 4.36 (d, J = 4.5 Hz, 1H), 4.18 (t, J = 2.5 Hz, 1H), 3.99 (ddd, J = 14.5, 9.0, 2.5 Hz, 1H), 3.19 (dt, J = 14.5, 3.1 Hz, 1H), 2.72 (d, J = 4.5 Hz, 3H), 0.95 (s, 9H), 0.70 (s, 9H), 0.15 (s, 3H), 0.13 (s, 3H), –0.13 (s, 3H), –0.49 (s, 3H); ^{13}C NMR ($CDCl_3$, 125 MHz) δ 159.1, 152.9, 151.0, 150.4, 150.3, 144.1, 137.1, 129.2, 125.0, 121.8, 121.2, 88.0, 87.8, 75.9, 73.5, 41.6, 26.8, 25.9, 25.6, 18.0, 17.7, –4.53, –4.79, –5.65; MS (FAB) *m/z* 671.3525 (MH^+ [$C_{31}H_{51}N_8O_5Si_2$]) = 671.3516.

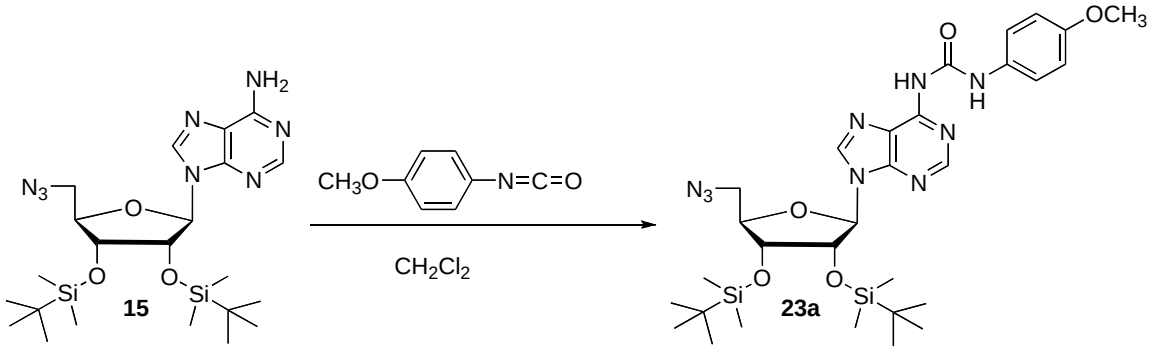

5´-Azido-2´,3´-bis-*O*-*tert*-butyldimethylsilyl-5´-deoxy-N^6-[*N*-(4-methoxyphenyl)-carbamoyl]adenosine (23a).

A solution of compound **15** (100 mg, 0.19 mmol) and 4-methoxyphenylisocyanate (0.24 mmol) in CH_2Cl_2 (2.4 mL) was stirred at ambient temperature until TLC indicated complete consumption of starting material (6 days). The crude reaction mixture was added directly to a flash chromatography column and eluted with 50% EtOAc/Hexanes to give **23a** (104 mg, 82%). ^{1}H NMR ($CDCl_3$, 500 MHz) δ 11.60 (s, 1H), 8.61 (s,1H), 8.53 (s, 1H), 8.36 (s, 1H), 7.54 (d, J = 8.8 Hz, 2H), 6.91 (d, J = 8.8 Hz, 2H), 5.98 (d, J = 4.5 Hz, 1H), 4.86 (t, J = 4.0 Hz, 1H), 4.32 (t, J = 4.5 Hz, 1H), 4.23 (dd, J = 9.5, 5.0 Hz, 1H), 3.82 (s, 3H), 3.72 (dd, J = 13.0, 4.0 Hz, 1H), 3.70 (dd, J = 13.0, 5.0 Hz, 1H), 0.94 (s, 9H), 0.84 (s, 9H), 0.13 (s, 3H), 0.11 (s, 3H), 0.00 (s, 3H), -0.16 (s, 3H); ^{13}C NMR ($CDCl_3$, 125 MHz) δ 156.3, 151.5, 150.8, 150.2, 150.1, 142.5, 131.0, 122.2, 121.2, 114.2, 89.7, 82.9, 74.7, 72.3, 55.5, 51.6, 25.8, 25.7, 18.0, 17.9, -4.4, -4.7, -4.85, -4.90; MS (ES) m/z ($[M+H]^+$ 670.3335 [$C_{30}H_{48}N_9O_5Si_2$] = 670.3317).

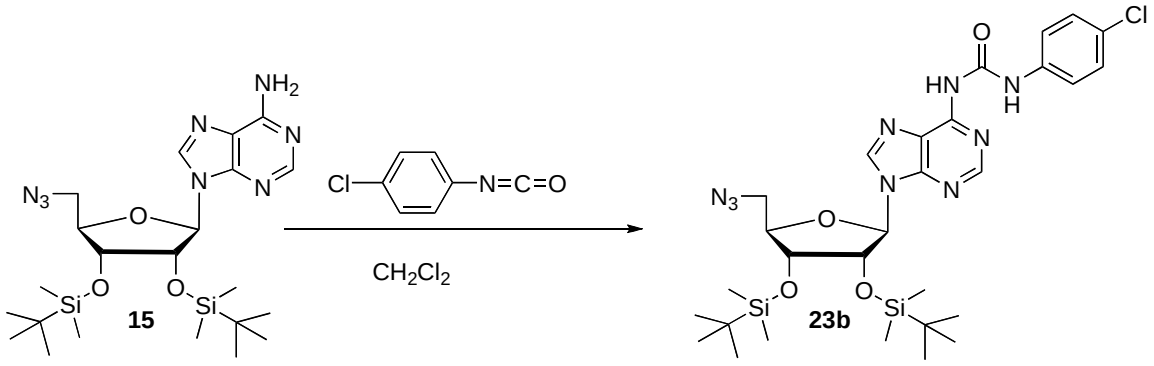

5´-Azido-2´,3´-bis-*O*-*tert*-butyldimethylsilyl-5´-deoxy-N^6-[*N*-(4-chlorophenyl)-carbamoyl]adenosine (23b).

A solution of compound **15** (60 mg, 0.12 mmol) and 4-chlorophenylisocyanate (0.14 mmol) in CH_2Cl_2 (1.8 mL) was stirred at ambient temperature until TLC indicated complete consumption of starting material (6 days). The crude reaction mixture was added directly to a flash chromatography column and eluted with 10% EtOAc/CH_2Cl_2 to give **23b** (40 mg, 50%). ^{1}H NMR ($CDCl_3$, 300 MHz) δ 11.91 (s, 1H), 8.81 (s,1H), 8.63 (s, 1H), 8.43 (s, 1H), 7.61 (d, J = 8.9 Hz, 2H), 7.32 (d, J = 8.9 Hz, 2H), 6.00 (d, J = 3.3 Hz, 1H), 4.85 (t, J = 4.2 Hz, 1H), 4.32 (t, J = 4.5 Hz, 1H), 4.23 (dd, J = 9.0, 4.8 Hz, 1H), 3.75 (dd, J = 13.1, 4.1 Hz, 1H), 3.69 (dd, J = 13.2, 4.8 Hz, 1H), 0.94 (s, 9H), 0.84 (s, 9H), 0.13 (s, 3H), 0.11 (s, 3H), 0.00 (s, 3H), -0.15 (s, 3H); ^{13}C NMR ($CDCl_3$, 75 MHz) δ 151.6, 150.9, 150.2, 143.0, 136.9, 129.2, 129.0, 121.7, 89.9, 83.1, 75.0, 72.5, 51.8, 26.00, 25.89, 18.26, 18.12, -4.17, -4.47, -4.63, -4.67; MS (ES) m/z ($[M+H]^+$ 674.2819 [$C_{29}H_{45}ClN_9O_4Si_2$] = 674.2816).

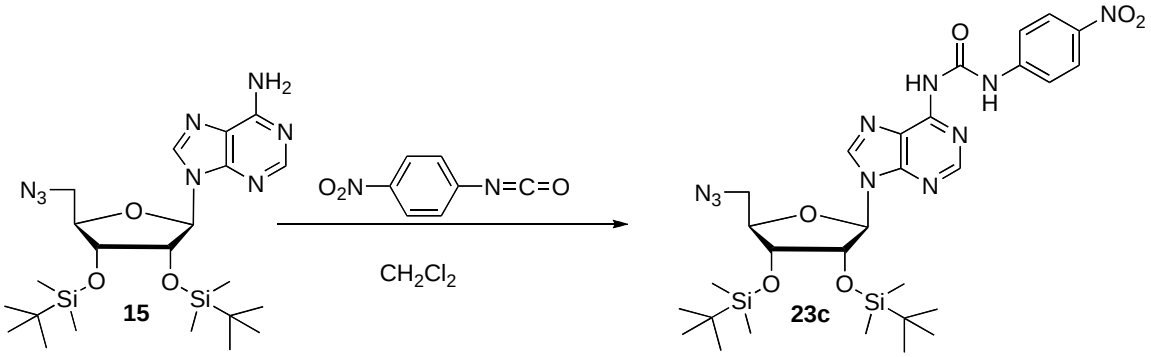

5´-Azido-2´,3´-bis-*O*-*tert*-butyldimethylsilyl-5´-deoxy-N^6-[*N*-(4-nitrophenyl)-carbamoyl]adenosine (23c).

A solution of compound **15** (100 mg, 0.20 mmol) and 4-nitrophenylisocyanate (0.24 mmol) in CH_2Cl_2 (2.4 mL) was stirred at ambient temperature until TLC indicated complete consumption of starting material (4 days). The crude reaction mixture was added directly to a flash chromatography column and eluted with 10% EtOAc/CH_2Cl_2 to give **23c** (97 mg, 71%). ^{1}H NMR ($CDCl_3$, 500 MHz) δ 12.39 (s, 1H), 8.69 (s, 1H), 8.64 (s, 1H), 8.38 (s, 1H), 8.27 (d, J = 9.3 Hz, 2H), 7.85 (d, J = 9.3 Hz, 2H), 6.02 (d, J = 4.5 Hz, 1H), 4.86 (t, J = 4.3 Hz, 1H), 4.33 (t, J = 4.3 Hz, 1H), 4.23 (dd, J = 8.7, 4.2 Hz, 1H), 3.77 (dd, J = 13.5, 4.0 Hz, 1H), 3.72 (dd, J = 13.5, 4.8 Hz, 1H), 0.95 (s, 9H), 0.85 (s, 9H), 0.14 (s, 3H), 0.13 (s, 3H), 0.02 (s, 3H), -0.14 (s, 3H); ^{13}C NMR ($CDCl_3$, 125 MHz) δ 151.2, 150.9, 150.7, 149.9, 144.4, 143.6, 143.0, 125.3, 121.6, 119.7, 90.0, 83.3, 75.1, 72.5, 51.8, 26.0, 25.9, 18.3, 18.1, -4.14, -4.42, -4.58, -4.67; MS 685.3057 (ES) m/z ($[M+H]^+$ $[C_{29}H_{45}N_{10}O_6Si_2]$ = 685.3062).

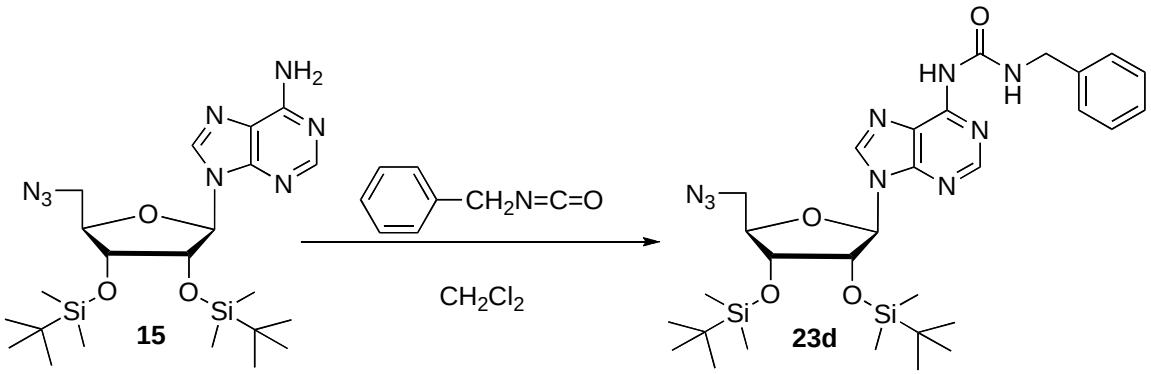

5´-Azido-2´,3´-bis-*O*-*tert*-butyldimethylsilyl-5´-deoxy-N^6-(*N*-benzylcarbamoyl)-adenosine (23d).

A solution of compound **15** (70 mg, 0.14 mmol) and benzylisocyanate (0.16 mmol) in CH_2Cl_2 (1.8 mL) was stirred at ambient temperature until TLC indicated complete consumption of starting material (8 days). The crude reaction mixture was added directly to a flash chromatography column and eluted with 10% EtOAc/CH_2Cl_2 to give **23d** (65 mg, 69%). ^{1}H NMR ($CDCl_3$, 300 MHz) δ 9.97 (bs, 1H), 8.78 (bs,1H), 8.48 (s, 1H), 8.42 (s,1H), 7.42-6.95 (m, 5H), 5.98 (d, J = 3.6 Hz, 1H), 4.83 (t, J = 4.2 Hz, 1H), 4.66 (d, J = 5.4 Hz, 2H), 4.34 (dd, J = 10.5, 5.1 Hz, 1H), 4.32 (t, J = 4.4 Hz, 1H), 4.22 (dd, J = 9.3, 4.5 Hz, 1H), 3.73 (dd, J = 13.8, 4.5 Hz, 1H), 3.66 (dd, J = 13.7, 5.0 Hz, 1H), 0.93 (s, 9H), 0.84 (s, 9H), 0.12 (s, 3H), 0.11 (s, 3H), 0.00 (s, 3H), -0.15 (s, 3H); ^{13}C NMR ($CDCl_3$, 75 MHz) δ 154.2, 151.0, 150.5, 142.4, 138.8, 128.6, 127.4, 127.3, 121.2, 89.7, 82.8, 74.8, 72.3, 51.6, 44.0, 29.8, 25.81, 25.70, 18.04, 17.90, -4.38, -4.70, -4.85; MS 654.3367 (ES) m/z ($[M+H]^+$ $[C_{30}H_{48}N_9O_4Si_2]$ = 654.3362).

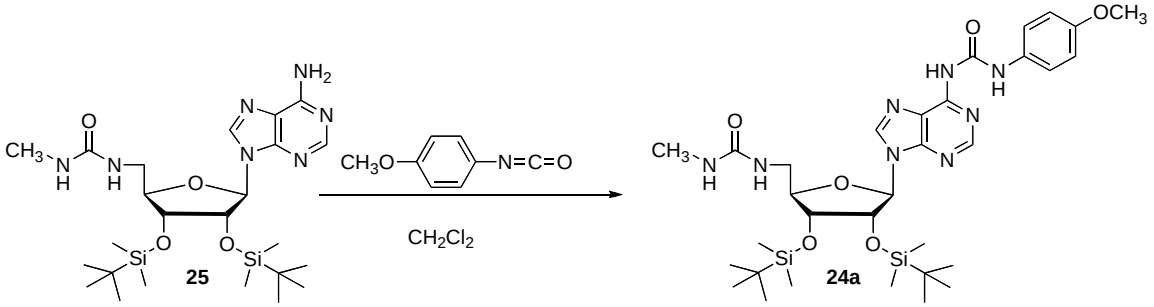

2´,3´-Bis-*O*-*tert*-butyldimethylsilyl-5´-deoxy-N^6-[*N*-(4-methoxyphenyl)carbamoyl]-5´-(*N*-methylcarbamoyl)aminoadenosine (24a).

A solution of **25** (80 mg, 0.14 mmol) and *p*-methoxyphenylisocyanate (0.17 mmol) in CH_2Cl_2 (1.74 mL) was stirred at ambient temperature and protected from moisture until the reaction was complete (6 d). The crude mixture was added directly to a flash chromatography column and eluted with 30% EtOAc/Hexanes → 4% MeOH/EtOAc to give **24a** (56 mg, 57 %). ^{1}H NMR (Acetone-d_6, 300 MHz) δ 11.98 (s, 1H), 9.55 (bs, 1H), 9.00 (s, 1H), 8.90 (s,1H), 7.67 (d, J = 9.0 Hz, 2H), 6.98 (d, J = 9.0 Hz, 2H), 6.40-6.32 (m, 1H), 6.19 (d, J = 7.5 Hz, 1H), 5.71 (d, J = 4.8 Hz, 1H), 4.97 (dd, J = 4.4, 7.4 Hz, 1H), 4.59 (d, J = 4.5 Hz, 1H), 4.19 (t, J=4.7 Hz, 1H), 3.83 (s, 3H), 3.77-3.67 (m, 1H), 3.62-3.54 (m, 1H), 2.72 (d, J = 4.2 Hz, 3H), 0.98 (s, 9H), 0.73 (s, 9H), 0.19 (s, 3H), 0.17 (s, 3H), 0.00 (s, 3H), -0.42 (s, 3H); ^{13}C NMR (Acetone-d_6, 75 MHz) δ 158.9, 156.3, 151.6, 151.4, 151.0, 150.9, 150.4, 143.9, 131.5, 131.4, 121.7, 121.6, 114.0, 87.9, 87.3, 75.2, 73.6, 54.8, 41.8, 25.5, 25.2, 17.8, 17.5, -5.14, -5.19, -5.33, -6.22; MS 701.3611 (ES) m/z ($[M+H]^+$ $[C_{32}H_{53}N_8O_6Si_2]$ = 701.3621).

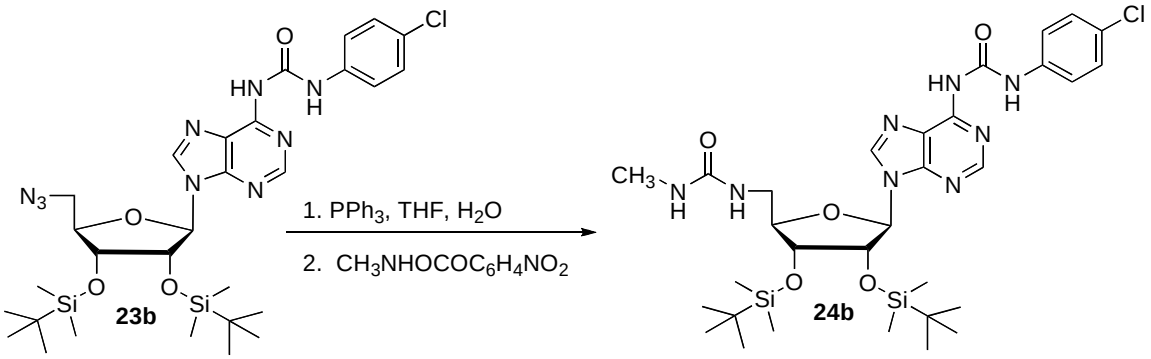

2´,3´-Bis-*O*-*tert*-butyldimethylsilyl-N^6-[*N*-(4-chlorophenyl)carbamoyl]-5´-deoxy-5´-(*N*-methylcarbamoyl)aminoadenosine (24b).

A solution of **23b** (60 mg, 0.09 mmol) and triphenylphosphine (35 mg, 0.13 mmol) in THF (0.6 mL) was stirred at ambient temperature for 15 min. Water (20 μL, 1.2 mmol) was added and the mixture was refluxed for 1.5 h at 85 °C. The resulting product was evaporated and chromatographed using EtOAc/CH_2Cl_2 /CH_3OH (4:2:1) to give the reduction product as a white powder. This product was mixed with *N*-methyl-*p*-nitro-phenylcarbamate (26 mg, 0.13 mmol) and triethylamine (50 μL, 0.36 mmol) in CH_2Cl_2 (2.3 mL) and stirred for 5 h at room temperature. Volatiles were removed under reduced pressure and the crude material was chromatographed using 30% acetone/hexanes→5% MeOH/CH_2Cl_2 to give **24b** (50 mg, 79%). ^{1}H NMR (Acetone-d_6, 300 MHz) δ 12.30 (s, 1H), 9.86 (s, 1H), 9.03 (s, 1H), 8.77 (s,1H), 7.79 (d, J = 9.0 Hz, 2H), 7.37 (d, J = 8.7 Hz, 2H), 6.34 (t, J = 6.0 Hz, 1H), 6.15 (d, J = 7.5 Hz, 1H), 5.74 (d, J = 5.1 Hz, 1H), 4.96 (dd, J = 4.4, 7.1 Hz, 1H), 4.54 (d, J = 4.2 Hz, 1H), 4.15 (t, J = 5.3 Hz, 1H), 3.70-3.60 (m, 2H), 2.72 (d, J = 4.5 Hz, 3H), 0.98 (s, 9H), 0.73 (s, 9H), 0.19 (s, 3H), 0.16 (s, 3H), -0.05 (s, 3H), -0.41 (s, 3H); ^{13}C NMR (Acetone-d_6, 75 MHz) δ 159.1, 151.5, 151.4, 151.0, 150.9, 150.2, 144.1, 137.6, 128.8, 128.5, 127.8, 121.3, 120.9, 87.9, 87.1, 75.2, 73.5, 41.9, 26.4,

26.3, 25.5, 25.3, 17.8, 17.5, -5.13, -5.19, -5.32, -6.16; MS 705.3126 (ES) *m*/*z* ($[M+H]^+$ $[C_{31}H_{51}N_8O_5Si_2]$ = 705.3145).

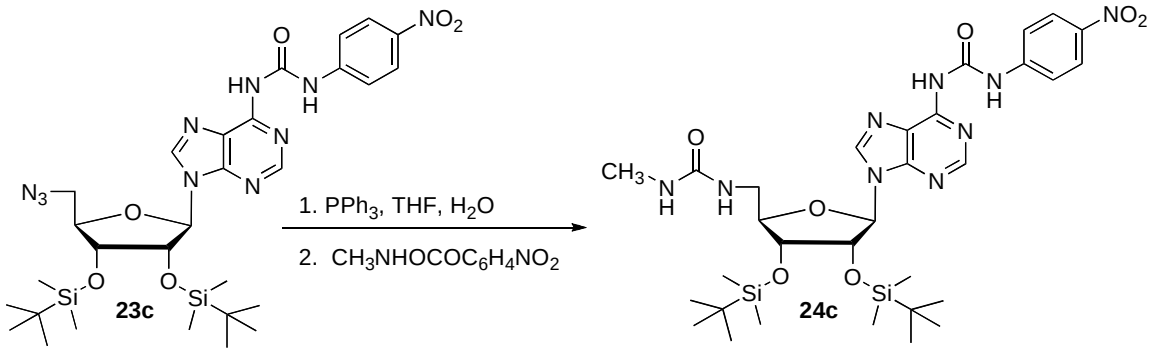

2´,3´-Bis-*O*-*tert*-butyldimethylsilyl-5´-deoxy-5´-(*N*-methylcarbamoyl)-N^6-[*N*-(4-nitrophenyl)carbamoyl]aminoadenosine (24c).

A solution of **23c** (50 mg, 0.09 mmol) and triphenylphosphine (29 mg, 0.11 mmol) in THF (0.5 mL) was stirred at ambient temperature for 15 min. Water (20 μL, 1.2 mmol) was added and the mixture was refluxed for 1.5 h at 85 °C. The resulting product was evaporated and chromatographed using EtOAc/CH_2Cl_2/CH_3OH (4:2:1) to give the reduction product as a white powder. This product was mixed with *N*-methyl-*p*-nitrophenylcarbamate (22 mg, 0.11 mmol) and triethylamine (40 μL, 0.29 mmol) in CH_2Cl_2 (1.9 mL) and stirred for 5 h at room temperature. Volatiles were removed under reduced pressure and the crude material was chromatographed using 30% acetone/hexanes→3% MeOH/CH_2Cl_2 to give **24c** (47 mg, 73%). ^{1}H NMR (Acetone-d_6, 300 MHz) δ 12.77 (s, 1H), 9.60 (s, 1H), 8.94 (s, 1H), 8.82 (s,1H), 8.26 (d, J = 9.3 Hz, 2H), 8.02 (d, J = 9.3 Hz, 2H), 6.33-6.30 (m, 1H), 6.14 (d, J = 7.6 Hz, 1H), 5.70 (d, J = 4.5 Hz, 1H), 5.00 (dd, J = 4.5, 2.7 Hz, 1H), 4.55 (d, J = 4.5 Hz, 1H), 4.15 (t, J = 5.4 Hz, 1H), 3.64 (d, J = 5.1 Hz, 2H), 2.74 (d, J = 4.2 Hz, 3H), 0.98 (s, 9H), 0.72 (s, 9H), 0.19 (s, 3H), 0.17 (s, 3H), -0.04 (s, 3H), -0.14 (s, 3H); ^{13}C NMR (Acetone-d_6, 75 MHz) δ 159.9, 152.2, 152.0, 151.8, 150.9, 145.9, 145.0, 143.9, 125.8, 122.0, 120.2, 120.1, 88.9, 88.1, 75.9, 74.4, 42.8, 42.7, 27.3, 27.1, 26.4, 26.1, 18.7, 18.4, -4.2, -4.3, -4.4, -5.3; MS 716.3366 (ES) m/z ($[M+H]^+$ $[C_{31}H_{50}N_9O_7Si_2]$ = 716.3353).

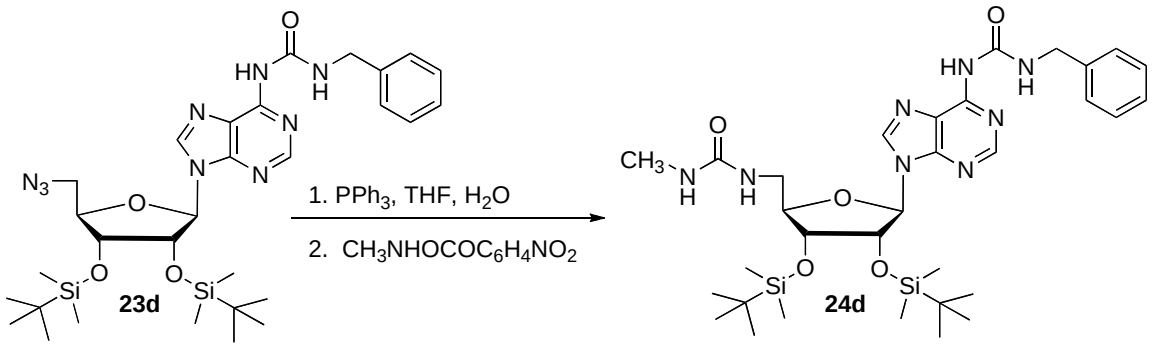

N^6-[*N*-Benzylcarbamoyl]-2´,3´-bis-*O*-*tert*-butyldimethylsilyl-5´-deoxy-5´-(*N*-methylcarbamoyl)aminoadenosine (24d).

A solution of **23c** (126 mg, 0.184 mmol) and triphenylphosphine (76 mg, 0.29 mmol) in THF (1.2 mL) was stirred at ambient temperature for 15 min. Water (45 μL, 2.5 mmol) was added and the mixture was refluxed for 1.5 h at 85 °C. The resulting product was evaporated and chromatographed using EtOAc/CH_2Cl_2/CH_3OH (4:2:1) to give the reduction product as a white powder. This product was mixed with *N*-methyl-*p*-nitrophenylcarbamate (57 mg, 0.29 mmol) and Na_2CO_3 (53 mg, 0.5 mmol) in EtOAc (8.0 mL), and stirred for 5 h at room temperature. Volatiles were removed under reduced pressure and the crude material was chromatographed using 30% acetone/hexanes → 3% MeOH/CH_2Cl_2 to give **24d** (65 mg, 52%). ^{1}H NMR ($CDCl_3$, 500 MHz) δ 10.43 (bs, 1H), 9.33 (bs, 1H), 8.91 (bs, 1H), 8.55 (s,1H), 7.39-7.36 (m, 3H), 7.32-7.29 (m, 2H), 6.34 (bs, 1H), 6.10 (d, J = 8.0 Hz, 1H), 5.27 (bs, 1H), 4.65 (d, J = 6.0 Hz, 2H), 4.49 (dd, J = 4.8, 7.8 Hz, 1H), 4.45 (d, J = 5.0 Hz, 1H), 4.13 (t, J = 5.4 Hz, 1H), 3.97 (ddd, J = 14.8, 8.0, 1.5 Hz, 1H), 2.97 (dt, J = 11.5, 3.0 Hz, 1H), 2.71 (d, J = 5.0 Hz, 3H), 0.96 (s, 9H), 0.69 (s, 9H), 0.15 (s, 3H), 0.14 (s, 3H), -0.12 (s, 3H), -0.49 (s, 3H); ^{13}C NMR ($CDCl_3$, 125 MHz) δ 159.5, 156.2, 151.7, 150.9, 150.5, 144.1, 138.2, 128.9, 127.6, 126.9, 120.8,

88.6, 86.6, 77.3, 73.9, 44.3, 41.5, 29.9, 26.9, 26.1, 25.7, 18.2, 17.9, -4.3, -4.6, -5.5; MS 685.3666 (ES) *m/z* ($[M+H]^+$ $[C_{32}H_{52}N_8O_5Si_2]$ = 685.3672).

Appendix

Developmental Therapeutics Program

One Dose Mean Graph

NSC: 749800 / 1	Conc: 1.00E-5 Molar	Test Date: Jan 26, 2009
Experiment ID: 0901OS41		Report Date: Feb 17, 2009

Panel/Cell Line	Growth Percent
Leukemia	
CCRF-CEM	57.37
HL-60(TB)	23.54
K-562	28.69
MOLT-4	34.33
RPMI-8226	39.74
Non-Small Cell Lung Cancer	
A549/ATCC	51.34
EKVX	67.49
HOP-62	77.38
HOP-92	62.10
NCI-H226	55.49
NCI-H23	81.04
NCI-H322M	91.13
NCI-H460	13.16
NCI-H522	45.31
Colon Cancer	
COLO 205	67.36
HCC-2998	-8.59
HCT-116	17.07
HCT-15	52.22
HT29	6.80
KM12	31.18
SW-620	72.19
CNS Cancer	
SF-268	59.89
SF-295	66.13
SF-539	33.37
SNB-19	99.06
SNB-75	45.42
U251	51.97
Melanoma	
LOX IMVI	46.64
MALME-3M	53.49
M14	57.11
MDA-MB-435	49.33
SK-MEL-2	59.98
SK-MEL-28	71.88
SK-MEL-5	23.48
UACC-257	58.16
UACC-62	65.12
Ovarian Cancer	
IGROV1	49.09
OVCAR-3	51.09
OVCAR-4	41.62
OVCAR-5	94.24
OVCAR-8	73.97
NCI/ADR-RES	48.06
SK-OV-3	94.67
Renal Cancer	
786-0	72.53
A498	77.42
ACHN	25.77
CAKI-1	60.80
RXF 393	34.96
SN12C	34.84
TK-10	87.72
UO-31	41.89
Prostate Cancer	
PC-3	32.41
DU-145	58.76
Breast Cancer	
MCF7	11.86
MDA-MB-231/ATCC	71.79
HS 578T	57.16
BT-549	64.46
T-47D	29.06
MDA-MB-468	61.90
Mean	52.35
Delta	60.94
Range	107.85

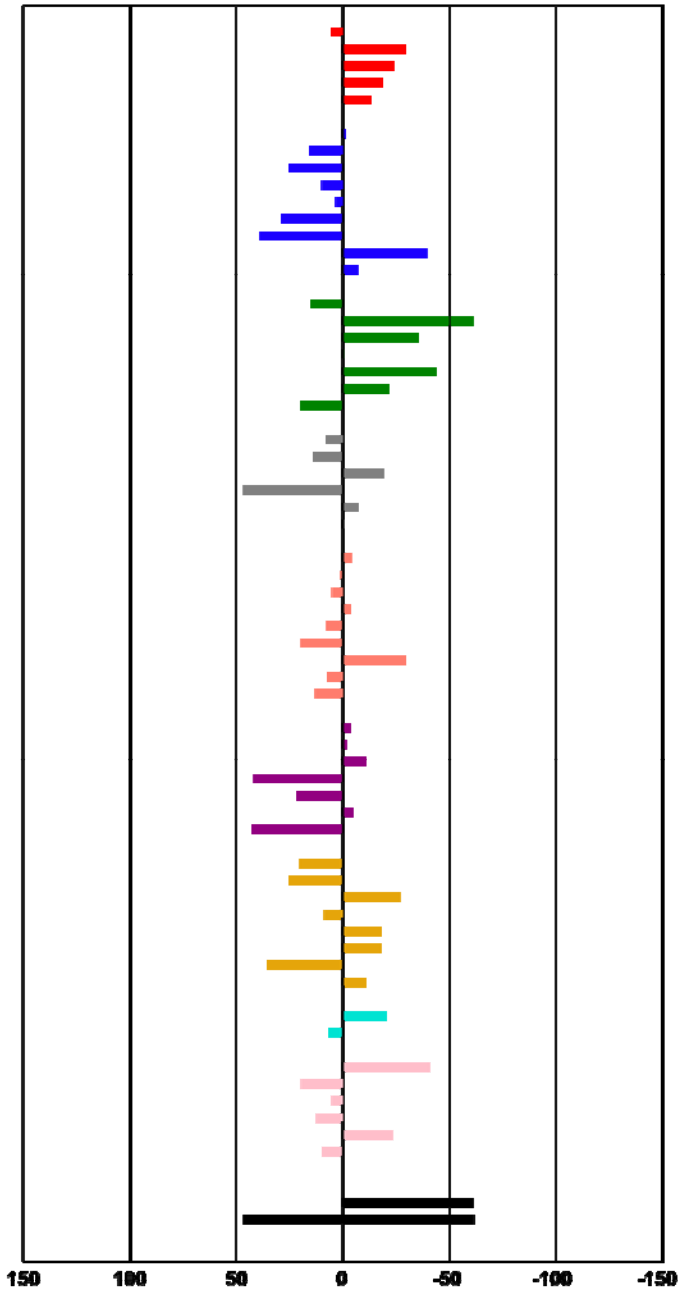

Developmental Therapeutics Program

One Dose Mean Graph

NSC: 749801 / 1	Conc: 1.00E-5 Molar	Test Date: Jan 26, 2009
Experiment ID: 0901OS41		Report Date: May 12, 2009

Panel/Cell Line	Growth Percent
Leukemia	
CCRF-CEM	98.21
HL-60(TB)	79.53
K-562	86.22
MOLT-4	55.48
RPMI-8226	78.80
Non-Small Cell Lung Cancer	
A549/ATCC	91.50
EKVX	82.97
HOP-62	73.98
HOP-92	95.17
NCI-H226	79.06
NCI-H23	104.57
NCI-H322M	98.90
NCI-H460	106.03
NCI-H522	75.08
Colon Cancer	
COLO 205	104.37
HCC-2998	55.41
HCT-116	80.53
HCT-15	86.54
HT29	99.88
KM12	102.44
SW-620	104.34
CNS Cancer	
SF-268	97.07
SF-295	92.38
SF-539	88.90
SNB-19	92.27
SNB-75	82.67
U251	86.08
Melanoma	
LOX IMVI	88.07
MALME-3M	98.42
M14	99.59
MDA-MB-435	95.55
SK-MEL-2	110.97
SK-MEL-28	105.54
SK-MEL-5	67.87
UACC-257	94.07
UACC-62	78.63
Ovarian Cancer	
IGROV1	118.36
OVCAR-3	97.77
OVCAR-4	78.30
OVCAR-5	114.49
OVCAR-8	97.90
NCI/ADR-RES	92.67
SK-OV-3	93.94
Renal Cancer	
786-0	87.13
A498	97.69
ACHN	89.04
CAKI-1	76.50
RXF 393	78.27
SN12C	95.84
TK-10	109.62
UO-31	95.07
Prostate Cancer	
PC-3	84.02
DU-145	99.79
Breast Cancer	
MCF7	98.33
MDA-MB-231/ATCC	85.45
HS 578T	93.32
BT-549	73.80
T-47D	84.46
MDA-MB-468	77.43
Mean	90.40
Delta	34.99
Range	62.95

Mean Growth Percent - Growth Percent

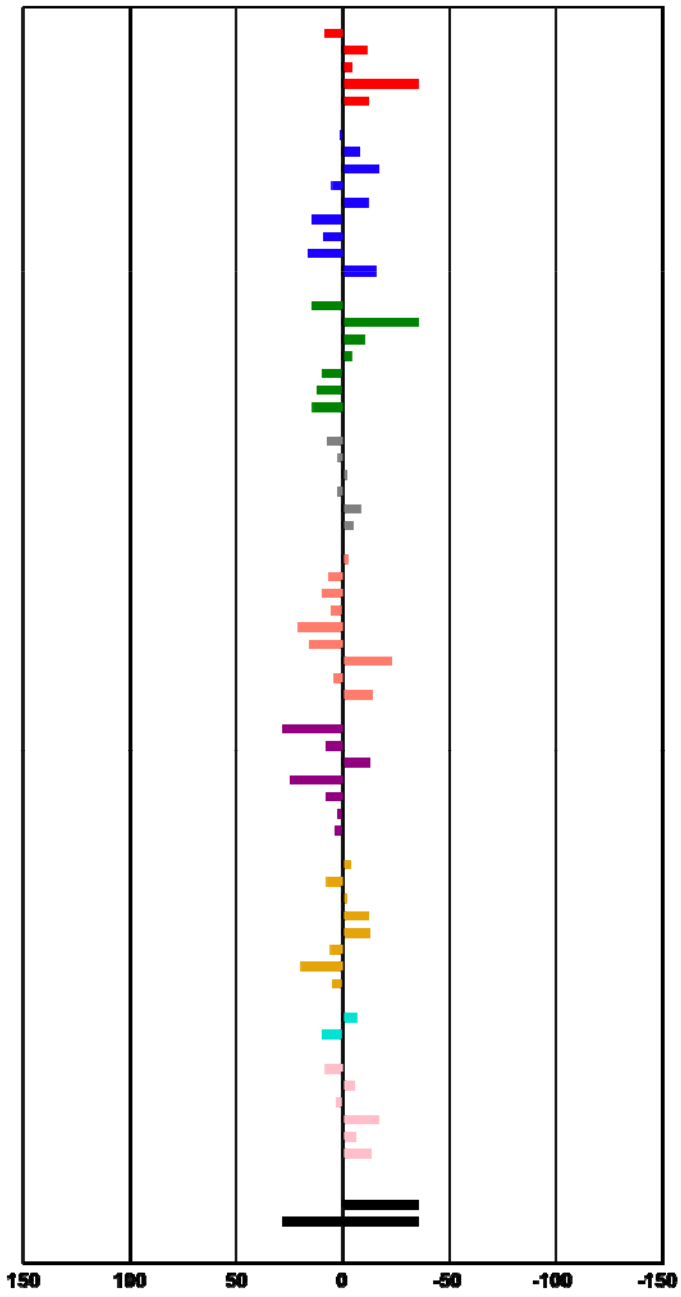

Developmental Therapeutics Program

One Dose Mean Graph

NSC: 749802 / 1	Conc: 1.00E-5 Molar	Test Date: Jan 26, 2009
Experiment ID: 0901OS41		Report Date: Feb 17, 2009

Panel/Cell Line	Growth Percent
Leukemia	
CCRF-CEM	97.54
HL-60(TB)	107.25
K-562	105.81
MOLT-4	108.66
RPMI-8226	97.59
Non-Small Cell Lung Cancer	
A549/ATCC	84.17
EKVX	92.43
HOP-62	83.91
HOP-92	94.41
NCI-H226	98.59
NCI-H23	97.38
NCI-H322M	93.82
NCI-H460	110.75
NCI-H522	79.23
Colon Cancer	
COLO 205	117.34
HCC-2998	83.79
HCT-116	99.80
HCT-15	96.58
HT29	111.09
KM12	102.46
SW-620	95.86
CNS Cancer	
SF-268	96.72
SF-295	101.19
SF-539	97.13
SNB-19	99.33
SNB-75	85.58
U251	98.45
Melanoma	
LOX IMVI	91.80
MALME-3M	95.44
M14	105.81
MDA-MB-435	95.08
SK-MEL-2	91.98
SK-MEL-28	107.33
SK-MEL-5	94.41
UACC-257	86.03
UACC-62	79.63
Ovarian Cancer	
IGROV1	96.53
OVCAR-3	98.00
OVCAR-4	99.93
OVCAR-5	86.80
OVCAR-8	100.16
NCI/ADR-RES	84.57
SK-OV-3	110.10
Renal Cancer	
786-0	93.43
A498	109.32
ACHN	90.08
CAKI-1	95.99
RXF 393	138.72
SN12C	87.75
TK-10	101.46
UO-31	87.28
Prostate Cancer	
PC-3	97.94
DU-145	97.70
Breast Cancer	
MCF7	84.01
MDA-MB-231/ATCC	98.74
HS 578T	97.70
BT-549	85.12
T-47D	94.66
MDA-MB-468	92.36
Mean	96.79
Delta	17.56
Range	59.49

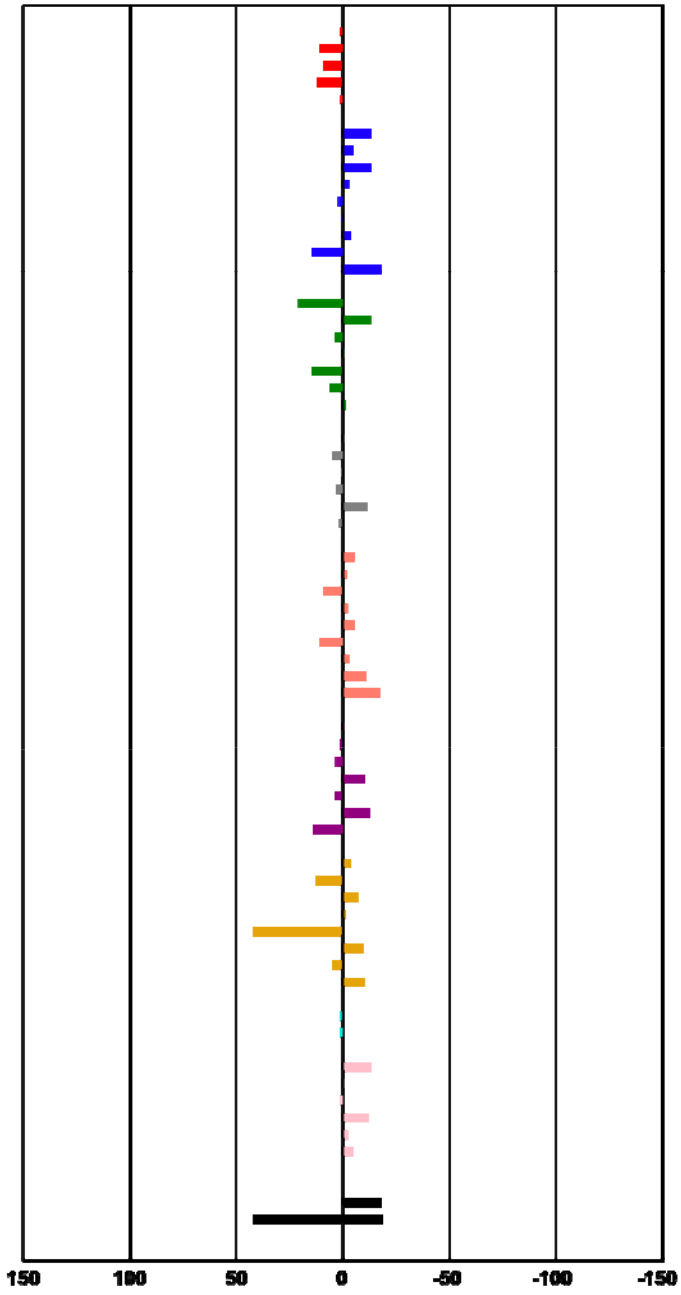

Developmental Therapeutics Program

One Dose Mean Graph

NSC: 749803 / 1	Conc: 1.00E-5 Molar	Test Date: Jan 26, 2009
Experiment ID: 0901OS41		Report Date: Feb 17, 2009

Panel/Cell Line	Growth Percent
Leukemia	
CCRF-CEM	62.87
HL-60(TB)	51.80
K-562	72.15
MOLT-4	78.70
RPMI-8226	75.12
Non-Small Cell Lung Cancer	
A549/ATCC	103.48
EKVX	88.93
HOP-62	98.39
HOP-92	99.99
NCI-H226	61.58
NCI-H23	97.42
NCI-H322M	99.43
NCI-H460	104.09
NCI-H522	89.98
Colon Cancer	
COLO 205	113.95
HCC-2998	120.91
HCT-116	81.91
HCT-15	84.37
HT29	103.48
KM12	100.76
SW-620	100.99
CNS Cancer	
SF-268	95.17
SF-295	93.68
SF-539	89.39
SNB-19	91.78
SNB-75	72.94
U251	94.82
Melanoma	
LOX IMVI	95.82
MALME-3M	97.34
M14	101.31
MDA-MB-435	92.90
SK-MEL-2	91.21
SK-MEL-28	116.10
SK-MEL-5	103.90
UACC-257	86.74
UACC-62	83.09
Ovarian Cancer	
IGROV1	92.56
OVCAR-3	111.18
OVCAR-4	88.25
OVCAR-5	107.33
OVCAR-8	97.90
NCI/ADR-RES	96.70
SK-OV-3	100.82
Renal Cancer	
786-0	89.17
A498	121.32
ACHN	92.04
CAKI-1	87.01
RXF 393	111.24
SN12C	80.88
TK-10	103.01
UO-31	82.53
Prostate Cancer	
PC-3	84.53
DU-145	105.69
Breast Cancer	
MCF7	84.70
MDA-MB-231/ATCC	95.33
HS 578T	91.81
BT-549	100.31
T-47D	73.08
MDA-MB-468	95.41
Mean	92.32
Delta	40.72
Range	69.72

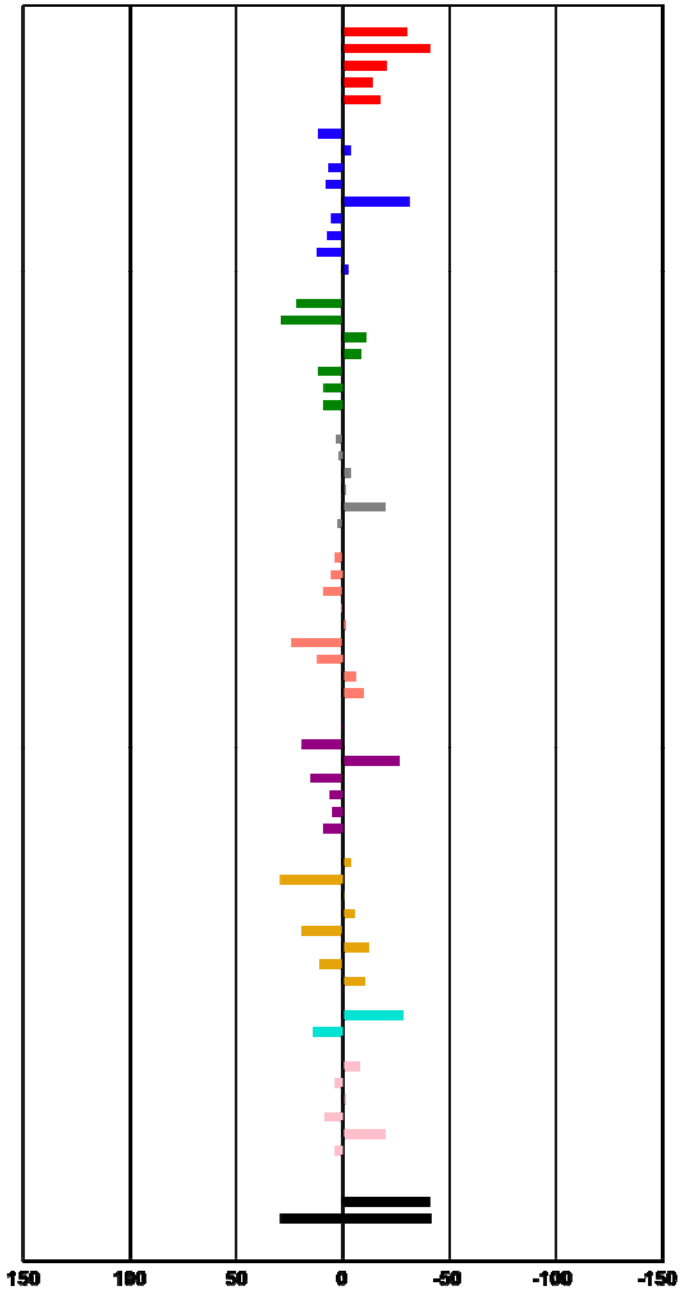

Developmental Therapeutics Program

One Dose Mean Graph

NSC: 749804 / 1	Conc: 1.00E-5 Molar	Test Date: Jan 26, 2009
Experiment ID: 0901OS41		Report Date: Feb 17, 2009

Panel/Cell Line	Growth Percent
Leukemia	
CCRF-CEM	82.88
HL-60(TB)	89.09
K-562	84.25
MOLT-4	74.47
RPMI-8226	98.55
Non-Small Cell Lung Cancer	
A549/ATCC	99.54
EKVX	74.63
HOP-62	91.22
HOP-92	81.19
NCI-H226	90.17
NCI-H23	108.99
NCI-H322M	90.94
NCI-H460	100.54
NCI-H522	91.91
Colon Cancer	
COLO 205	106.54
HCC-2998	104.23
HCT-116	93.94
HCT-15	90.99
HT29	97.72
KM12	108.99
SW-620	103.24
CNS Cancer	
SF-268	97.48
SF-295	97.20
SF-539	90.58
SNB-19	102.88
SNB-75	75.14
U251	98.82
Melanoma	
LOX IMVI	91.48
MALME-3M	92.89
M14	99.28
MDA-MB-435	94.64
SK-MEL-2	108.09
SK-MEL-28	112.23
SK-MEL-5	80.73
UACC-257	104.48
UACC-62	73.05
Ovarian Cancer	
IGROV1	89.71
OVCAR-3	98.00
OVCAR-4	98.41
OVCAR-5	101.19
OVCAR-8	102.58
NCI/ADR-RES	90.21
SK-OV-3	103.18
Renal Cancer	
786-0	97.21
A498	97.94
ACHN	101.85
CAKI-1	92.38
RXF 393	111.67
SN12C	84.48
TK-10	94.18
UO-31	72.31
Prostate Cancer	
PC-3	85.21
DU-145	92.65
Breast Cancer	
MCF7	89.23
MDA-MB-231/ATCC	89.81
HS 578T	101.90
BT-549	76.66
T-47D	82.17
MDA-MB-468	94.14
Mean	93.68
Delta	21.37
Range	39.92

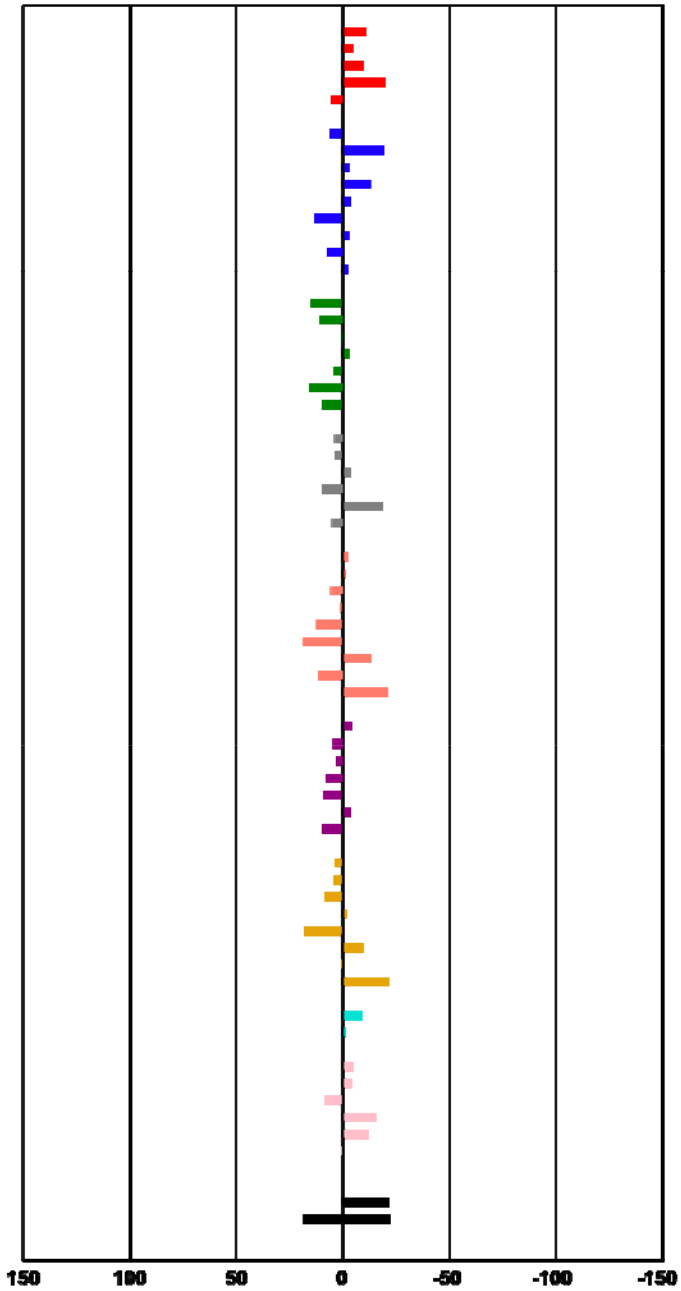

Developmental Therapeutics Program

One Dose Mean Graph

NSC: 749805 / 1	Conc: 1.00E-5 Molar	Test Date: Jan 26, 2009
Experiment ID: 0901OS41		Report Date: Feb 17, 2009

Panel/Cell Line	Growth Percent
Leukemia	
CCRF-CEM	116.66
HL-60(TB)	75.94
K-562	83.69
MOLT-4	75.38
RPMI-8226	80.65
Non-Small Cell Lung Cancer	
A549/ATCC	99.55
EKVX	85.84
HOP-62	96.81
HOP-92	90.02
NCI-H226	90.13
NCI-H23	99.17
NCI-H322M	81.08
NCI-H460	109.73
NCI-H522	74.14
Colon Cancer	
COLO 205	76.25
HCC-2998	70.97
HCT-116	52.05
HCT-15	90.13
HT29	65.08
KM12	60.12
SW-620	88.23
CNS Cancer	
SF-268	96.33
SF-295	88.15
SF-539	92.05
SNB-19	88.05
SNB-75	97.53
U251	53.55
Melanoma	
LOX IMVI	73.84
MALME-3M	104.66
M14	86.71
MDA-MB-435	67.46
SK-MEL-2	93.59
SK-MEL-28	111.32
SK-MEL-5	74.94
UACC-257	95.45
UACC-62	79.04
Ovarian Cancer	
IGROV1	48.12
OVCAR-3	65.44
OVCAR-4	71.01
OVCAR-5	88.41
OVCAR-8	103.63
NCI/ADR-RES	89.32
SK-OV-3	101.78
Renal Cancer	
786-0	76.74
A498	78.45
ACHN	69.58
CAKI-1	84.74
RXF 393	104.64
SN12C	90.29
TK-10	84.88
UO-31	75.80
Prostate Cancer	
PC-3	92.49
DU-145	70.86
Breast Cancer	
MCF7	94.25
MDA-MB-231/ATCC	81.35
HS 578T	106.80
BT-549	79.80
T-47D	79.15
MDA-MB-468	70.83
Mean	84.34
Delta	38.22
Range	72.54

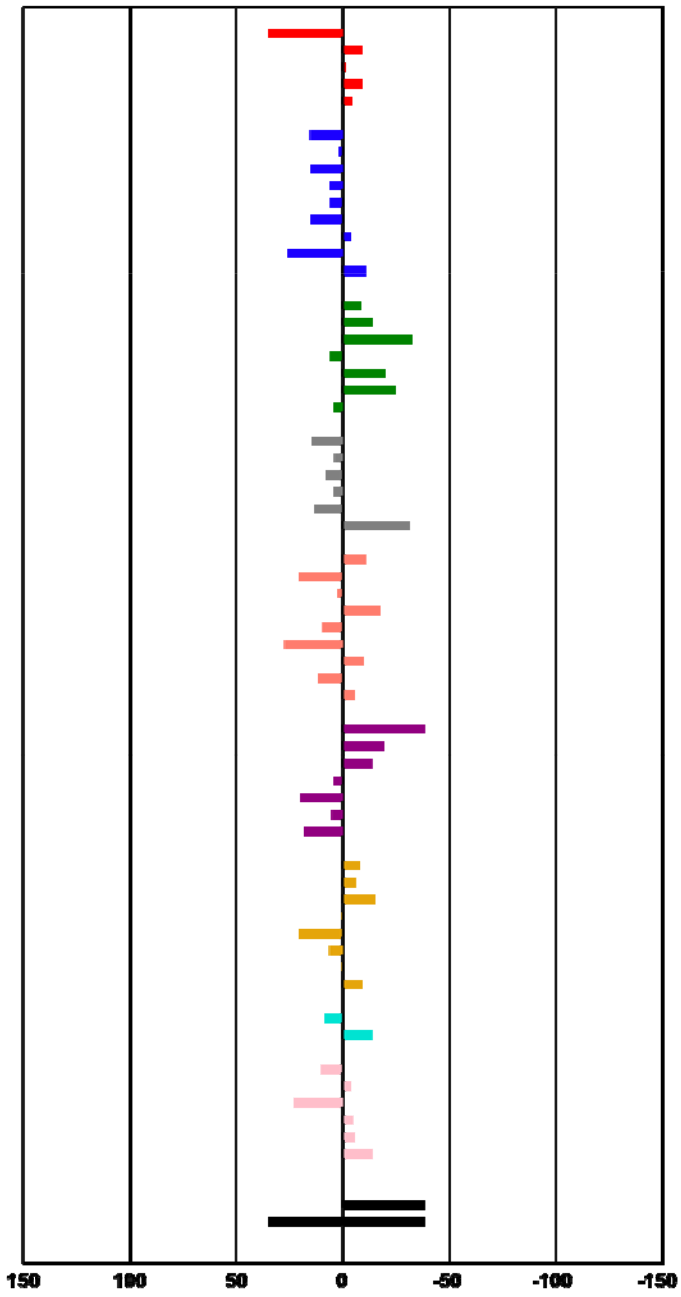

Developmental Therapeutics Program

One Dose Mean Graph

NSC: 750689 / 1	Conc: 1.00E-5 Molar	Test Date: Jul 06, 2009
Experiment ID: 0907OS76		Report Date: Oct 22, 2009

Panel/Cell Line	Growth Percent
Leukemia	
CCRF-CEM	42.61
HL-60(TB)	23.46
K-562	34.49
MOLT-4	24.10
RPMI-8226	20.22
SR	-22.06
Non-Small Cell Lung Cancer	
A549/ATCC	22.99
EKVX	23.44
HOP-62	61.74
HOP-92	-2.68
NCI-H226	49.05
NCI-H23	36.34
NCI-H322M	87.32
NCI-H460	-6.74
NCI-H522	46.16
Colon Cancer	
COLO 205	-100.00
HCC-2998	-1.37
HCT-116	0.33
HCT-15	21.33
HT29	-67.72
KM12	-3.66
SW-620	36.35
CNS Cancer	
SF-268	35.99
SF-295	45.14
SF-539	33.40
SNB-19	76.11
SNB-75	45.81
U251	17.24
Melanoma	
LOX IMVI	13.27
MALME-3M	48.88
M14	32.98
MDA-MB-435	25.94
SK-MEL-2	56.73
SK-MEL-28	60.01
SK-MEL-5	48.21
UACC-257	42.80
UACC-62	41.90
Ovarian Cancer	
IGROV1	52.53
OVCAR-3	-28.71
OVCAR-4	29.63
OVCAR-5	69.19
OVCAR-8	32.85
NCI/ADR-RES	31.03
SK-OV-3	77.55
Renal Cancer	
786-0	16.53
ACHN	20.53
CAKI-1	59.49
RXF 393	-36.96
SN12C	-79.29
TK-10	34.25
UO-31	48.26
Prostate Cancer	
PC-3	7.78
DU-145	52.18
Breast Cancer	
MCF7	0.29
MDA-MB-231/ATCC	37.66
HS 578T	60.99
BT-549	39.72
T-47D	13.64
MDA-MB-468	35.78
Mean	25.85
Delta	125.85
Range	187.32

Mean Growth Percent - Growth Percent

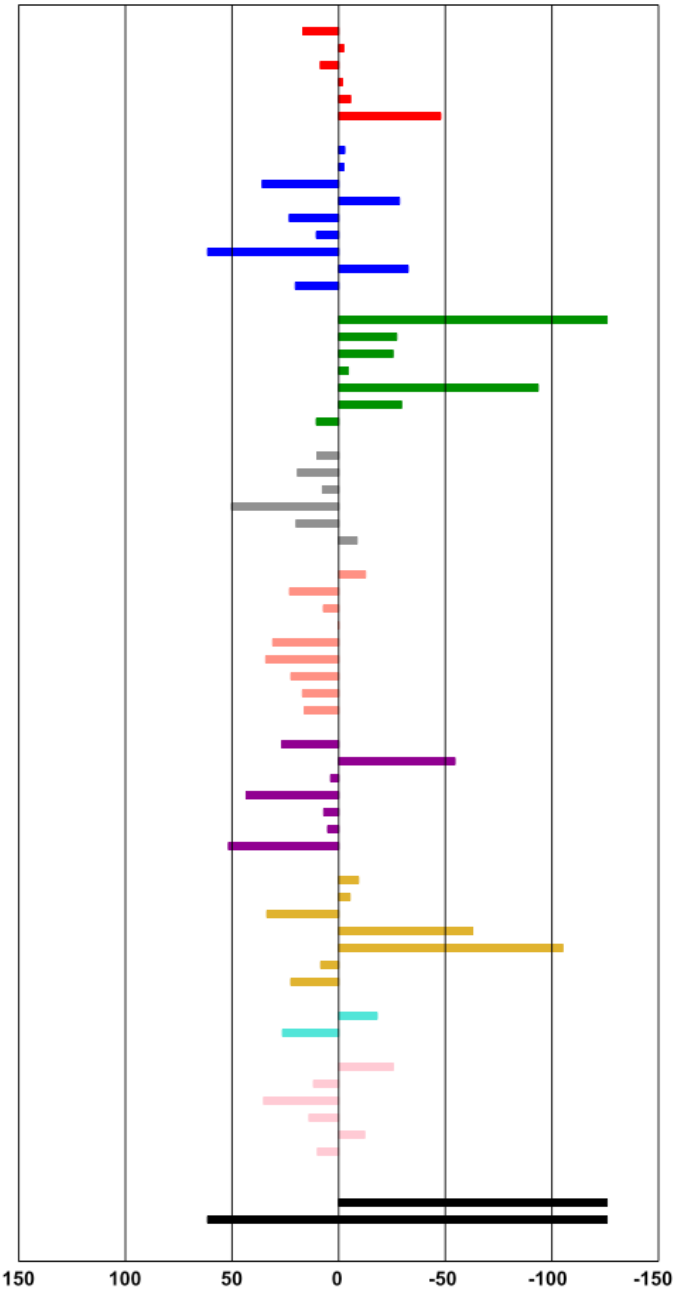

References:

[1] Pawson, T. Protein molecules and signaling networks, *Nature* **1995**, 373, 573–580.

[2] (a) Egan, S. E.; Weinberg, R. A. The pathway to signal achievement, *Nature* **1993**, *365*, 781– 782; (b) Blume-Jensen, P.; Hunter, T. Oncogenic kinase signaling, *Nature* **2001**, *411*, 355– 365; (c) Hanahan, D.; Weinberg, R. A. The hallmarks of cancer, *Cell* **2000**, *100*, 57– 70.

[3] Dancey, J.; Sausville, E. Issues and progress with protein kinase inhibitors for cancer treatment, *Nat Rev Drug Discovery* **2003**, *2*, 296–313.

[4] (a) Michael, W. N.; Deininger M.; Druker, B. J. Specific Targeted Therapy Of Chronic Myelogenous Leukemia With Imatinib, *Pharmacol. Reviews.* **2003**, *55*, No. 3, (b) Kantarjian, H.; Kurzrock, R.; Talpaz, M. Philadelphia chromosome-negative chronic myelogenous leukemia and chronic myelomonocytic leukemia, *Hematol. Oncol. Clin. North Am.* **1990**, *4*, 389–404.

[5] Kantarjian, H. M.; Cortes J. New Strategies In Chronic Myeloid Leukemia. *Int. J. Hematology,* **2006**, *83*, 289–293

[6] Deininger, M.; Druker, B. J. Specific Targeted Therapy of Chronic Myelogenous Leukemia with Imatinib, *Pharmacol Rev*. **2003**, 55(3), 401–423,

[7] Sordella, R.; Bell, D.; Haber, D.; Settleman, J. Gefitinib-Sensitizing EGFR Mutations in Lung Cancer Activate Anti-Apoptotic Pathways, *Science*, **2004**, *305*, 1163-1167.

[8] Tsao, M. Sakurada, A.; Cutz, J. C.; Zhu, C. Q.; Kamel-Reid, S.; Squire, J.; Lorimer, I.; Zhang, T.; Liu, N.; Daneshmand, M.; Marrano, P.; Santos, G. D.; Lagarde, A.; Richardson, F.; Seymour, L.; Whitehead, M.; Ding, K. Y.; Pater, J.; Shepherd, F. A.

Erlotinib in Lung Cancer — Molecular and Clinical Predictors of Outcome, *New Eng. J. Med.* **2005**, *353*, 133–144.

[9] (a) Fabbro, D.; Ruetz, S.; Buchdunger, E.; Cowan-Jacob, S. W.; Fendrich, G.; Liebetanz, J.; Mestan, J.; O'Reilly, T.; Traxler, P.; Chaudhuri, B.; Fretz, H.; Zimmerman, J.; Meyer, T.; Caravatti, G.; Furet, P.; Manley, P. W. Protein Kinases as Targets for Anticancer Agents: From Inhibitors to Useful Drugs, *Pharm. Ther.* **2002**, *93*, 79–98.

[10] Peterson, M. A.; Ke, P.; Shi, H.; Jones, C.; McDougall, B. R.; Robinson, W. E. Design, Synthesis, and Antiviral Evaluation of Some 3'-Carboxymethyl-3'-Deoxyadenosine Derivatives, *Nucleos. Nucleotid. Nucl.* **2007**, *26*, 499–519.

[11] Vichai, V.; Kirtikara, K. Sulorhodamine B colorimetric assay for cytotoxicity screening, *Nature Protocols.* **2006**, *1*, 1112–1116.

[12] Paull, K. D.; Shoemaker, R. H.; Hodes, L.; Monks, A.; Scudiero, D. A.; Rubinstein, L.; Plowman, J.; Boyd, M. R. Display and Analysis of Patterns of Differential Activity of Drugs Against Human Tumor Cell Lines: Development of Mean Graph and COMPARE Algorithm, *J. Natl. Cancer Inst.* **1989**, *81*, 1088–92.

[13] Ambit Biosciences. March, 2009 <http://www.ambitbio.com/>

[14] Fabian, M.A.; Biggs, W. H. III; Treiber, D. K.; Atteridge, C. E.; Azimioara, M. D.; Benedetti, M. G.; Carter, T. A.; Ciceri, P.; Edeen, P. T.; Floyd, M.; Ford, J. M.; Galvin, M.; Gerlach, J. L.; Grotzfeld, R. M.; Herrgard, S.; Insko, D. E.; Insko, M. A.; Lai, A. G.; Lélias, J.-M.; Mehta, S. A.; Milanov, Z. V.; Velasco, A. M.; Wodicka, L. M.; Patel, H. K.; Zarrinkar, P. P.; Lockhart, D. J . A Small Molecule-Kinase Interaction Map for Clinical Kinase Inhibitors, *Nature Biotech*. **2005**, *23*, 329–336.

[15] Peterson, M. A.; Oliveira, M.; Christiansen, M. A.; Cutler, C. E. Preliminary SAR Analysis of Novel Antiproliferative N6,5'-Bis-ureidoadenosine Derivatives, *Bioorg. Med. Chem. Lett.* **2009**, *19*, 6775–6779.

[16] Karaman, M. W.; Herrgard, S.; Treiber, D. K.; Gallant, P.; Atteridge, C. E., Campbell, B. T.; Chan, K. W.; Ciceri, P.; Davis, M. I.; Edeen, P. T.; Faraoni, R.; Floyd, M.; Hunt, J. P.; Lockhart, D. J.; Milanov, Z. V.; Morrison, M. J.; Pallares, G.; Patel, H. K.; Pritchard, S.; Wodicka, L. M.; Zarrinkar, P. P. A Quantitative Analysis of Kinase Inhibitor Selectivity, *Nature Biotech.* **2008**, *26*, 127–132.

[17] (a) Helms, M. W.; Packeisen, J.; August, C.; Schittek, B.; Boecker, W.; Brandt, B. H.; Buerger, H. First Evidence Supporting a Potential Role for the BMP/SMAD Pathway in the Progression of Oestrogen Receptor-positive Breast Cancer, *J. Pathol.* **2005**, *206*, 366–376.

(b) Alarmo, E.-L.; Kuukasjärvi, T.; Karhu, R.; Kallioniemi, A. A Comprehensive Expression Survey of Bone Morphogenetic Proteins in Breast Cancer Highlights the Importance of BMP4 and BMP7. *Breast Cancer Res. Treat.* **2007**, *103*, 239–246.

[18] Anderson, G. J.; Darshan, D. Small-Molecule Dissection of BMP Signaling, *Nature Chem. Biol.* **2008**, *4*, 15–16.

[19] Peterson, M. A.; Shi, H.; Ke, P. A Simple and Efficient Biphasic Method for the Preparation of 4-Nitrophenyl *N*-Methyl- and *N*-Alkylcarbamates, *Tetrahedron Lett*. **2006**, *47*, 3405–3407.